

Two-dimensional Ising-like systems: Corrections to scaling in the Klauder and double-Gaussian models

Mustansir Barma* and Michael E. Fisher

Baker Laboratory, Cornell University, Ithaca, New York 14853

(Received 27 August 1984)

Partial-differential approximants are used to study the critical behavior of the susceptibility, $\chi(x,y)$, of the Klauder and double-Gaussian scalar spin, or $O(1)$ models on a square lattice using two-variable series to order x^{21} where $x \propto J/k_B T$ while y serves to interpolate analytically from the Gaussian or free-field model at $y=0$ to the standard spin- $\frac{1}{2}$ Ising model at $y=1$. The pure Ising critical point at $y=1$ appears to be the only non-Gaussian multisingularity in the range $0 < y \leq 1$. It is concluded that the exponent θ characterizing the leading irrelevant corrections to scaling lies in the range $\theta = 1.35 \pm 0.25$. This supports the validity of Nienhuis's conjecture $\theta = \frac{4}{3}$ but it is argued that, contrary to normal expectations, this (rational) value entails only logarithmic corrections to pure Ising critical behavior. The existence of strong crossover effects for $0.1 \leq y \leq 0.6$ and the appearance of an effective exponent, $\gamma_{\text{eff}} \simeq 1.9$ to 2.0, is discussed and related to work on the $\lambda\varphi^4$ model.

I. INTRODUCTION

When a critical point is approached, there are always corrections to the leading power-law singularities of various thermodynamic quantities. For instance, the susceptibility $\chi(T)$ of a ferromagnet near its critical temperature T_c is typically expected to be¹ of the form

$$\chi \approx Ct^{-\gamma}(1 + a_1 t + a_2 t^2 + \cdots + a_\theta t^\theta + a_{\theta+1} t^{\theta+1} + a_{2\theta} t^{2\theta} + \cdots + a_\theta t^\theta + a_{\theta+1} t^{\theta+1} + \cdots), \quad (1.1)$$

where

$$t = (T - T_c)/T_c \quad (1.2)$$

is the reduced temperature. The leading critical exponent γ , and the correction exponents θ, θ', \dots , are expected to be universal, while the amplitudes C and a_i are expected to depend smoothly on any subsidiary parameters which may change T_c , but do not affect the nature of the transition. The general structure of (1.1) is predicted by renormalization-group theory,¹ which also identifies two distinct sources of correction terms. First, the full *scaling fields* are *nonlinear* functions of observable fields like t , and their expansion normally yields integral powers of t . Second, *irrelevant operators* at the pertinent fixed point give rise to independent, and, in general, nonanalytic, contributions represented by powers of t with nonintegral exponents θ, θ' , etc.

For Ising-like, i.e., scalar spin or $O(1)$ critical systems in $d=3$ spatial dimensions, the existence of strong leading nonanalytic corrections described by $\theta \simeq 0.5$ is quite well established. The first evidence came from renormalization-group $\epsilon=4-d$ expansions extrapolated to $d=3$ ($\epsilon=1$) which can be done with reasonable confidence.²⁻⁵ Then came field-theoretic perturbation calculations performed in $d=3$ dimensions for a $\lambda\varphi^4$ Lagrangian.^{6,4} A careful analysis of long series⁷ for the Ising model of general spin S on a body-centered-cubic lattice

has been presented by Zinn-Justin.⁸ By assuming that γ and θ are independent of S (a very plausible but arguable hypothesis), the series analyses could be appropriately "biased." Values of θ in good accord with the field-theoretic approaches were obtained.⁹

Finally, Chen, Fisher, and Nickel¹⁰ have reported an *unbiased* analysis of *double* series to order x^{21} , with $x \propto J/k_B T$, for the susceptibility, $\chi(x,y)$, of the Klauder and double-Gaussian models on a bcc lattice. These continuous-spin models,¹⁰ which are explained in detail in Sec. II, interpolate analytically from the pure Gaussian model, or free-field lattice theory, at $y=0$ to the standard spin- $\frac{1}{2}$ Ising model (the *pure* Ising model) at $y=1$. Chen *et al.* analyzed the susceptibility $\chi(x,y)$ with the aid of *partial-differential-approximant* (PDA) techniques,^{11,12} which utilize the full two-variable nature of the power series in an essential way. In particular, the method can address the question of the number of distinct universality classes arising in a model. Moreover, PDAs can accommodate nonlinear scaling fields naturally, thereby focusing directly on corrections arising from irrelevant operators. The analysis of Chen *et al.*¹⁰ indicated that, within the Klauder (KI) and double-Gaussian (DG) models, the critical behavior is always Ising-like for $0 < y \leq 1$. For the correction exponent they obtained the estimate $\theta = 0.54 \pm 0.05$. This value agrees well with the results of Zinn-Justin for the spin- S Ising model⁸ and with the ϵ expansion and field-theoretic estimates.^{6,4} The theoretical situation in $d=3$ dimensions is, thus, in a rather satisfactory state.

Paradoxically, the situation in $d=2$ dimensions has been much less clear despite the availability of many exact results for the pure spin- $\frac{1}{2}$ Ising model.¹³⁻¹⁵ Accordingly, in this paper we address the question of corrections to scaling in two-dimensional Ising-like systems by studying the Klauder and double-Gaussian models on a square lattice where again, thanks to Nickel,¹⁶ the series are known to order x^{21} .

Before outlining our work and its conclusions, it is appropriate to review what may be said about the problem on the basis of the current literature. One must note, first, that exact calculations for the magnetic susceptibility, $\chi_I(T)$, of the pure, square lattice Ising model near criticality¹⁵ have, so far, revealed only *analytic* corrections to the leading power law. As discussed by Aharony and Fisher,¹⁷ it seems that these can be fully and consistently accounted for in terms of nonlinear scaling fields involving only t and the (reduced) magnetic field $h = H/k_B T$. Nonlinear fields in the $d=2$ Ising model should also yield¹⁷ an additive singularity to $\chi_I(T)$ of the form $t \ln |t|$ [beyond terms shown in (1.7)], but this lies at a higher order than is available in the present exact calculations.¹⁵ However, *no evidence* has been seen in any of the exact expressions for corrections to leading behavior that can be identified with irrelevant operators with *nonintegral* exponents, θ .

In view of these results one may ask: "Can a nonintegral correction exponent, θ , arise in two-dimensional ferromagnetic systems, like the K1 and DG models, which differ from the pure Ising model but which otherwise should be in the same universality class?" This might be possible if the corresponding correction amplitudes, a_i , happened to vanish identically in the case of a pure Ising model. This would imply that the Onsager critical point embodied some special symmetry or lay on some special manifold in the space of all scalar spin Hamiltonians—a circumstance which should not be so surprising in view of the exact solvability of the pure Ising models. If the pure Ising limit is special in this way, however, we can still ask for the exponent θ characterizing the leading nonanalytic corrections to scaling in scalar spin models which deviate from the limit. Presumably such corrections should also arise and be detectable in real physical systems in the Ising-like universality class.

At present no firm answers to this question have been advanced. However, by an ingenious series of mappings, not all of which are exact, Nienhuis¹⁸ has transformed the q -state Potts model in two dimensions into a Gaussian model with spatially staggered fields. On setting $q=2$ to recapture the Ising model, he was led to conclude that $\theta = \frac{4}{3}$ describes one of the correction exponents in Ising-like models. In order to reconcile this result with the known behavior of the Ising model, which, as we have mentioned, appears not to display any such corrections, Nienhuis argued that the corresponding operator might be associated only with *derivatives* with respect to q ; if so, the irrelevant variable describing an exponent with this value of θ might well not be observable in models which belong to the Ising ($q=2$) universality class.

Recently, by postulating conformal covariance and unitarity at criticality, Friedan, Qui, and Shenker¹⁹ have found sets of critical exponents for infinitely many $d=2$ models; their analysis exhibits no scaling operator with exponent $\theta = \frac{4}{3}$ in the Ising-like case. However, one may presume that if there were natural operators within the full Ising-like universality class that violated unitarity (as may antiferromagnetic spin-spin couplings) or conformal covariance (although at present this seems less likely), then such operators would not show up in the analysis of

Friedan, Qui, and Shenker. Indeed, there is an intriguing hint of the value $\theta = \frac{4}{3}$ in the work of Andrews, Baxter, and Forrester.²⁰ They have solved exactly two infinite sequences of two-dimensional solid-on-solid-like lattice models. As Huse²¹ has pointed out, the exponents of one of their sequences agree with all those found by Friedan *et al.*;¹⁹ the other sequence is not included in their results. Further, for a class of multicritical points describing n -phase coexistence their solutions yield²¹ a correction exponent

$$\theta_n = (n+2)/(n+1). \quad (1.3)$$

This formula applies, strictly, only for $n \geq 3$, but if one sets $n=2$ (in accord with two-phase coexistence below a normal Ising critical point) one finds $\theta_2 = \frac{4}{3}$ in conformity with Nienhuis's conclusion for θ !

Despite the elusive nature of the singular corrections in exact work pertaining to the pure Ising model, there is some evidence which suggests $\theta \simeq \frac{4}{3}$ in studies of various two-dimensional systems expected to be in the Ising universality class. In the first instance one may extrapolate the renormalization-group ϵ expansions to $d=2$ ($\epsilon=2$): This is a rather uncertain procedure, but it yields⁴ $\theta \simeq 1.4$. The perturbative calculations for $\lambda\phi^4$ field theory in two dimensions by Baker, Nickel, and Meiron^{6(b)} gave²² $\theta = 1.4 \pm 0.8$, which was refined by Le Guillou and Zinn-Justin⁴ to $\theta = 1.3 \pm 0.2$, in remarkable agreement, considering the technical difficulties, with Nienhuis's (later) work. Moreover, a recent study by Adler and Enting²³ of long series for the spontaneous magnetization and low-temperature susceptibility of the spin-1 Ising model on a square lattice and for the hard square-lattice gas suggests $1 < \theta < 1.3$. However, one might, looking at their best series data, conclude $\theta \simeq 1.18$, but, as must be stressed, it is extremely difficult in *any single-variable* analysis in which T_c is not known exactly to disentangle reliably the effects of irrelevant operators from those due to the nonlinear scaling fields (which give rise to $\theta_{\text{eff}}=1$).¹ Privman²⁴ has analyzed finite-size data due to Debierre and Turban²⁵ for hard "triangles" (on a hexagonal lattice) and found evidence for $\theta \simeq 1.13$ to 1.15, but with uncertainties of ± 0.20 . Again, we take this as no more than indicative of some nontrivial corrections in Ising-like systems characterized by θ in, say, the range 1.1 to 1.5.

As we explain below, our own PDA study of the square-lattice Klauder and double-Gaussian model also suggests results fully consistent with Nienhuis's conjecture $\theta = \frac{4}{3}$. More concretely, we conclude²⁶ that in the (x,y) plane specifying the K1 and DG models, the pure Ising critical point is the only non-Gaussian multisingularity, and further that the Ising limit, $y \equiv 1$, represents a scaling axis. We then find,²⁶ with a high degree of confidence, that there are corrections characterized by

$$\theta = 1.35 \pm 0.25. \quad (1.4)$$

However, we go on, in Sec. V, to show that it is possible to understand the meaning of a nonintegral correction exponent θ , despite the absence of appropriate nonintegral powers of t in the correction-to-scaling factors, provided θ is a *rational* fraction. Of course, $\theta = m/n$ with $m=4$ and

$n=3$, is fully consistent with (1.4) and identical with Nienhuis's value! Our arguments invoke Wegner's powerful analysis¹ of corrections to scaling in renormalization-group flows and suggest that θ controls the appearance of logarithmic terms in the correction factors for models in the Ising universality class when $d=2$.

Our study also addresses another theoretical issue. It is commonly held that the $\lambda\varphi^4$ lattice model is always in the same universality class as the pure Ising model, but this view has been challenged, particularly by Baker and Johnson.²⁷ In recent work these authors studied the $\lambda\varphi^4$ lattice model in two dimensions for a particular "border" value, $\lambda=\lambda_B$, of the coupling constant, using single-variable series. The value λ_B had been identified in previous analytical work by Baker^{27(b)} as apparently playing a special role in the correspondence between continuum and lattice field theories. On the basis of their single-variable analysis Baker and Johnson concluded that the $\lambda\varphi^4$ models encompass a new, *non-Ising* universality class with a susceptibility exponent $\gamma\approx 2.0$. (For comparison, recall that $\gamma=1\frac{3}{4}$ for the Ising model.²⁸) Now we find, in Sec. II, that single-variable studies of the double-Gaussian and Klauder models also suggest an effective exponent, γ_{eff} , in the range 1.9 to 2.0 for $y\approx 0.5$ and 0.3 for the two models, respectively. However, our PDA study indicates, and we believe quite convincingly, that the true critical behavior of both models is Ising-like for all $0<y\leq 1$, so that the observation of $\gamma_{\text{eff}}\approx 2.0$ for intermediate values of y merely represents a nonasymptotic value resulting from crossover effects. Because of the quantitative similarities of the DG and K1 models to the $\lambda\varphi^4$ model, it seems likely to us that these conclusions apply equally to that model. We present some evidence, however, that the strong crossover effects seen in the K1, DG, and $\lambda\varphi^4$ models result from the presence of a *tricritical* manifold which, in the full space of scalar spin Hamiltonians, lies "close" to the models studied.

To conclude this Introduction we outline the plan of the paper. The Klauder and double-Gaussian models are defined in Sec. II and various relationships between them are discussed; in particular, the perturbation theory for both models around the Ising and Gaussian limits is developed: the first-order results are identical at the Ising limit. The construction of appropriate partial-differential approximants for two-variable series expansions for both models is described in Sec. III, specifically as regards the imposition of constraints along the Gaussian and Ising axes, $y=0$ and $y=1$. The results of our PDA analysis are discussed in Sec. IV where the evidence for our various conclusions is marshalled. In Sec. V, as mentioned, we discuss the special features of renormalization-group flows that arise when θ is rational. Finally, in Sec. VI we present some evidence to support of the association of the "border" models with incipient tricriticality. Our conclusions are summarized briefly in Sec. VII.

II. THE DOUBLE-GAUSSIAN AND KLAUDER MODELS

The partition functions of both the double-Gaussian¹⁰ and Klauder²⁹ models are computed by integrating over

continuous-spin variables s_i in $(-\infty, \infty)$ to obtain

$$Z_X(T; y) = \int \prod_i ds_i W_X(s_i; y) \exp(-\mathcal{H}/k_B T), \quad (2.1)$$

where the subscript X stands for DG (double Gaussian) or K1 (Klauder). The Hamiltonian is given in both cases by

$$\mathcal{H} = - \sum_{(i,j)} J_{ij} s_i s_j, \quad (2.2)$$

where the sum runs over all pairs of sites (i, j) on the given lattice, and J_{ij} is the coupling between spins s_i and s_j at spatial separation \mathbf{R}_{ij} . In later sections, we will deal specifically with a square lattice with pairwise coupling J_{ij} between only nearest-neighbor sites; but most of the formulas in this section hold equally in the general case. The single-site spin weight functions $W_X(s; y)$ are different for the two models: Specifically, we have¹⁰

$$W_{\text{DG}} \propto b(e^{-(s-\sqrt{y})^2/2g} + e^{-(s+\sqrt{y})^2/2g}), \quad (2.3)$$

$$W_{\text{K1}} \propto b |s|^{y/g} e^{-s^2/2g}, \quad (2.4)$$

where for convenience here and later we have set³⁰

$$g \equiv 1 - y \quad \text{and} \quad b^2 \equiv 1/2(1 - y). \quad (2.5)$$

Both weight functions clearly interpolate analytically between a pure Gaussian form at $y=0$, which specifies a free-field lattice model, to a standard spin- $\frac{1}{2}$ Ising form (sum of two delta functions at $s=\pm 1$) at $y=1$.

For computational purposes it is useful to know the cumulants, $\mu_n^X(y)$, of the weight functions. These are defined, as usual, through the partition function for a single spin in a field: Specifically, we have

$$\begin{aligned} Z_X^0(h; y) &\equiv \int_{-\infty}^{\infty} ds e^{hs} W_X(s; y) \\ &= \exp \left[\sum_{n=0}^{\infty} \mu_n^X(y) h^n / n! \right]. \end{aligned} \quad (2.6)$$

By symmetry all the odd-order cumulants vanish. The weight functions (2.3) and (2.4) have been constructed to satisfy

$$\mu_2^{\text{DG}}(y) = \mu_2^{\text{K1}}(y) = 1, \quad (2.7)$$

a property which can be checked straightforwardly. Since μ_2^X is equal to $\langle s^2 \rangle_X^0$, the mean-square value of a noninteracting ($T=\infty$) spin, and since this in turn determines the mean-field critical temperature $T_c^0(y)$, the normalization (2.7) ensures that the mean-field critical temperatures are *independent* of y and equal for both models: Explicitly, we have

$$k_B T_c^0 = \sum_{j \neq i} J_{ij} \equiv \hat{J}(0). \quad (2.8)$$

Now it can be shown quite easily³¹ that the partition function of the double-Gaussian model factorizes exactly into the partition function of a simple Gaussian model with reduced couplings

$$K'_{ij} = K_{ij} - \delta_{ij}/g \quad \text{where} \quad K_{ij} = J_{ij}/k_B T \quad (J_{ii} \equiv 0), \quad (2.9)$$

and a spin- $\frac{1}{2}$ Ising model with longer-range (reduced) interactions $L_{ij} = J_{ij}^R/k_B T$, a so-called "range" model.³² Explicitly, one finds

$$Z_{\text{DG}}(\mathbf{K}) = Z_G(\mathbf{K}') Z_R(\mathbf{L}), \quad (2.10)$$

where the Fourier transform,

$$\hat{L}(\mathbf{q}) = \sum_j e^{-i\mathbf{q} \cdot \mathbf{R}_{ij}} L_{ij}, \quad (2.11)$$

of the new interactions is given in terms of $\hat{K}(\mathbf{q})$ (defined similarly) by

$$\hat{L}(\mathbf{q}) = y \hat{K}(\mathbf{q}) / [1 - g \hat{K}(\mathbf{q})]. \quad (2.12)$$

Note that in the Ising limit, $g=0$, the range model reduces simply to the original pure Ising model ($y=1$) with Hamiltonian \mathcal{H}_I given by (2.2) with $s_i = \pm 1$, while the Gaussian model becomes trivial since $s_i \equiv 0$ is enforced by (2.9).

It follows from this transformation that the double-Gaussian model exhibits two distinct transition loci. At fixed, positive y the transition associated with the range model occurs at a higher temperature than that arising from the Gaussian partition function. Indeed, the DG model ceases to be defined below the Gaussian transition since the partition function, Z_G , then diverges. The associated region of stability is given by

$$g \hat{K}(0) = (1-y) T_c^0 / T \leq 1. \quad (2.13)$$

(See Fig. 2, below, which shows the stability boundary and the coincident critical loci of the DG and range models.)

The factorization (2.10) allows one to define an analytic continuation of the double-Gaussian model, including its correlation functions, beyond the two physical boundaries at $y=0$ and $y=1$. However, the range model itself becomes undefined if the denominator in (2.12) changes sign. For nearest-neighbor interactions on a bipartite lattice [for which $\min_{\mathbf{q}} \hat{K}(\mathbf{q}) = -\hat{K}(0)$] this yields a complementary boundary lying in the region for $y > 1$ and specified by

$$|g| \hat{K}(0) = (y-1) T_c^0 / T = 1. \quad (2.14)$$

No corresponding factorization property or analytic continuation has (as yet) been found for the Klauder model, but, like the DG model, it also is defined only in the region (2.13). Nonetheless an unexpected exact relationship between the two models emerges on considering small deviations around the Ising limit, $y=1$. The essential result is that *to linear order in $g=1-y$* the thermodynamic properties of both models even in the presence of a nonzero magnetic field are *identical* provided one adopts the correspondence

$$g_{\text{KI}} = 2g_{\text{DG}}. \quad (2.15)$$

This result can be established most conveniently by proving that all the cumulants $\mu_n^{\text{DG}}(y)$ and $\mu_n^{\text{KI}}(y)$ of the single-spin weight factors for the two models agree to leading order under (2.15). This in turn follows from the identity

$$\begin{aligned} Z_{\text{DG}}^0(h; 1-g) &= (\cosh h) [1 + \frac{1}{2} g h (h - \tanh h) + O(g^2)] \\ &= Z_{\text{KI}}^0(h; 1-2g) [1 + O(g^2)] \end{aligned} \quad (2.16)$$

for the normalized single-spin partition functions [see (2.6)]. This is proved in Appendix A.

Now, if we also use the equivalence of the DG model to a Gaussian plus a range model we have, to leading order in g ,

$$\begin{aligned} Z_{\text{DG}}(1-g) &\approx Z_{\text{KI}}(1-2g) \\ &\approx e^{-Ng} \sum_{\{s_i\}} \exp\{-[\mathcal{H}_I(\{s_i\}) + g \mathcal{D}(\{s_i\})] / k_B T\}, \end{aligned} \quad (2.17)$$

where N is the number of lattice sites while $\mathcal{H}_I(\{s_i\})$ denotes the original ($y=1, g=0$) pure spin- $\frac{1}{2}$ Ising Hamiltonian with $s_i = \pm 1$ (all i). The perturbation Hamiltonian, $\mathcal{D}(\{s_i\})$, arises from the range-model potentials as defined through (2.12) and may, hence, be written explicitly without much effort. If we specialize to a square lattice and restrict the interactions to nearest-neighbor site pairs, $\langle ij \rangle$, with $J_{ij} = J$ we obtain

$$\mathcal{D} = -J \sum_{\langle ij \rangle} s_i s_j + \mathcal{D}_1(\{s_i\}), \quad (2.18)$$

where from (2.12) one finds, with $K = J / k_B T$,

$$\mathcal{D}_1 / k_B T \equiv \overline{\mathcal{D}}_1 = 4NK^2 + 2K^2 \sum_{\langle ij \rangle_2} s_i s_j + K^2 \sum_{\langle ij \rangle_3} s_i s_j, \quad (2.19)$$

in which $\langle ij \rangle_k$ denotes pairs of k th-nearest-neighbor sites (as measured geometrically by $|\mathbf{R}_{ij}|$). The coefficients 4, 2, and 1 in this result represent the number of distinct two-step lattice walks from the origin, O , back to O , from O to the next-nearest site, and from O to the next-nearest-neighbor (nnn) site, respectively. Thus, to first order in g both the DG and KI models are equivalent to a spin- $\frac{1}{2}$ Ising model with only first-, second-, and third-neighbor interactions. (Note that this result holds, modulo some small differences in geometry, for any space lattice.)

The full susceptibility of the double-Gaussian model can be expressed as the sum of terms arising from the simple Gaussian and range factors in (2.10). One finds^{32,33}

$$\chi_{\text{DG}} = \frac{g}{1 - g \hat{K}(0)} + \frac{y}{[1 - g \hat{K}(0)]^2} \chi_R, \quad (2.20)$$

where χ_R is the susceptibility of the range model. On treating the term $g \mathcal{D}_1$ in (2.18) as a perturbation and using the correspondence (2.15), we find, to first order in g ,

$$\begin{aligned} \chi_{\text{KI}}(2g) &= \chi_{\text{DG}}(g) = \chi_{yI} [1 + g(8K - 1)] + g \\ &\quad + g \sum_i (\langle s_0 s_i \overline{\mathcal{D}}_1 \rangle_{yI} - \langle s_0 s_i \rangle_{yI} \langle \overline{\mathcal{D}}_1 \rangle_{yI}), \end{aligned} \quad (2.21)$$

where χ_{yI} is the susceptibility of an Ising Hamiltonian with nearest-neighbor couplings yJ and the thermal averages are computed for the same Hamiltonian.

Finally, let us consider the approach of the DG and KI models to the *Gaussian limit*, $y=0$. By using the equivalence to decoupled Gaussian and range models, we find^{32,33}

$$\chi_{\text{DG}}(x,y) = \frac{1}{1-x} - y^2 \frac{I(x)-1}{(1-x)^2} + O(y^3), \quad (2.22)$$

where, for use here and below, we have set

$$x = \hat{J}(0)/k_B T = T_c^0/T. \quad (2.23)$$

The transcendental function $I(x)$ in (2.22) is defined by

$$I(x) = \frac{1}{(2\pi)^d} \int \frac{d^d q}{1 - x \hat{K}(\mathbf{q})/\hat{K}(\mathbf{0})}. \quad (2.24)$$

For nearest-neighbor interactions on a simple- or body-centered-cubic lattice, this reduces to a Watson integral; on a nearest-neighbor square lattice it can be expressed directly in terms of the complete elliptic integral as $2K(2x)/\pi$, and in that case, one has

$$\pi I(x) \approx -\ln[8(1-x)] \quad \text{as } x \rightarrow 1-. \quad (2.25)$$

For the Klaunder model, no corresponding equivalence to simpler decoupled models is known, but Nickel³² has observed a symmetry property in the dependence of the cumulants on y . Explicitly, one finds the results

$$\begin{aligned} \mu_4^{\text{Kl}} &= (-2)y, \\ \mu_6^{\text{Kl}} &= 2(-2)^2 y(1+y), \\ \mu_8^{\text{Kl}} &= 2(-2)^3 y(3+11y+3y^2), \\ \mu_{10}^{\text{Kl}} &= 8(-2)^4 y(3+28y+28y^2+3y^3), \end{aligned} \quad (2.26)$$

which seem to follow the rule

$$\mu_{2n+2} = (-2)^n y(n! + \dots + n!y^{n-1}), \quad (2.27)$$

in which the polynomial factor is symmetric under reversal of its coefficients. Now to leading order in perturbation theory about the Gaussian limit, $y=0$, the linear term in y is required in each cumulant. If one accepts the conjecture (2.27), one can thus establish³²

$$\chi_{\text{Kl}}(x,y) = \frac{1}{1-x} + \frac{y[I(x)-1]}{(1-x)^2 I(x)} + O(y^2). \quad (2.28)$$

In contrast to the limit $y \rightarrow 1$, we see, by comparing with (2.22), that there is no simple relation between the Kl and DG models when $y \rightarrow 0$. However, as regards the dominant $(1-x)^{-2}$ correction to the Gaussian susceptibility, $\chi_G = (1-x)^{-1}$, we see that the appropriate scaling field around the Gaussian multicritical point is y for the Kl model but y^2 for the DG model. This suggests that one make the general identification

$$y_{\text{Kl}} = y_{\text{DG}}^2 \quad (2.29)$$

in comparing properties of the two models. This relation actually implies the Ising limit correspondence (2.15) (to leading order). Furthermore, it *also* leads to the precise equality of the fourth-order cumulants for the two models³⁴ since, in comparison with (2.26), one has

$$\mu_4^{\text{DG}}(y) = -2y^2, \quad \mu_6^{\text{DG}}(y) = 16y^3, \quad \mu_8^{\text{DG}} = -272y^4, \quad \dots \quad (2.30)$$

Evidently the correspondence (2.29) is not exact (which it clearly could not be); nevertheless, it embodies a most useful approximate mapping between the two models and we will adopt it in making comparisons.

As a last comment on the general nature of the two models we may compare the DG model with $\lambda\varphi^4$ lattice field theory, which corresponds to a spin weight factor of the form

$$W_{\lambda\varphi^4} \propto \exp(-\frac{1}{2}u_2 s^2 - \frac{1}{24}u_4 s^4), \quad (2.31)$$

with $\lambda \propto u_4$. One finds

$$u_2 \propto (1-2y)/(1-y)^2 \quad \text{and} \quad \lambda, u_4 \propto y^2/(1-y)^4, \quad (2.32)$$

although in the DG model there are, of course, also higher-order terms varying as s^k which have amplitudes $u_k \propto [y/(1-y)^2]^k$. On the other hand, because of the nonanalytic factor $|s|^{y/g}$ in the Kl model weight factor one cannot make such a small s comparison with the $\lambda\varphi^4$ model. Indeed, we may attribute the different nature of the leading corrections to χ_G in the DG and Kl models (which, for $d=2$, diverge as $\Delta\chi \sim (1-x)^{-2} \ln(1-x)$ and $(1-x)^{-2} [1+c/\ln(1-x)]$, respectively; see (2.22) and (2.28)) to this same difference. Other models with weight factors analytic in x as $s \rightarrow 0$ should yield similar results to the DG model near the Gaussian limit.

III. SERIES ANALYSIS

Away from the Gaussian and Ising limits, no exact results are known for the critical behavior of the susceptibility, $\chi(x,y)$, of the square-lattice Klaunder and double-Gaussian models. However, Nickel¹⁶ has derived double power series in the inverse temperature, $x=4J/k_B T$, and in the parameter y for both models. With the aid of proper extrapolation techniques, one may hope to use these series to learn about the critical and multicritical behavior of the models. In this section and the next, we describe our analysis using partial-differential approximants (PDAs),^{11,12} which, as mentioned, capitalize on the two-variable character of the series at hand.

A. Single-variable analysis

Before turning to the PDA study, it is appropriate to examine the results of a single-variable analysis of $\chi(x,y)$. At a fixed value of y , the double power series for χ reduces to an expansion in the variable x , which can then be studied by established techniques such as D log Padé approximants³⁵ and inhomogeneous differential approximants.³⁶ The estimates for the exponents γ and the critical points $x_c(y)$, resulting from such fixed- y scans taken at intervals $\Delta y = 0.1$, are summarized graphically in Fig. 1. Notice that, in conformity with the remarks at the end of the preceding section, the estimates for the Kl and DG models are plotted versus y_{Kl} and y_{DG}^2 , respectively. As expected, the estimated critical points for the two models are quite close to one another over the whole range of y . Note that, since the series are long and fairly regular, the dispersions in the estimates of $x_c(y)$ from approximant to approximant are quite negligible on the scale of the graph.

The estimates for γ must be regarded, at least in the first instance, as *effective exponents*, $\gamma_{\text{eff}}(y)$, for two

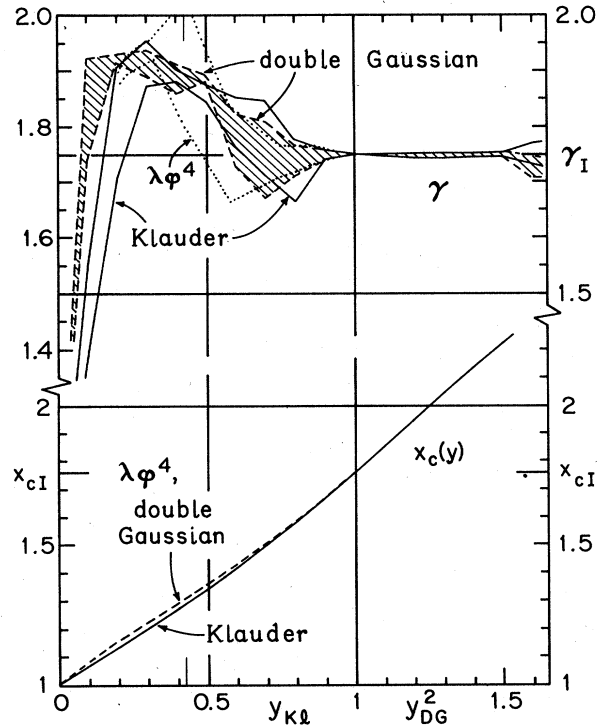


FIG. 1. The results of single-variable D log Padé and inhomogeneous differential approximant analysis for γ and x_c are shown for the Klauder and double-Gaussian models at intervals $\Delta y_{Kl} = \Delta y_{DG}^2 = 0.1$. The spread in the value of the effective exponent is obtained by taking the largest and smallest values of γ found from some 20 approximants, after eliminating outliers. The results (dotted) for the $\lambda\varphi^4$ model have been plotted so that the values of x_c agree with those for the DG model: the "border" model is located at ordinate 0.425.

reasons: First, the D log Padé and inhomogeneous differential approximants make no specific allowance for singular correction factors and, second, one knows there must be strong crossover effects in *some* range of y since the exponent must cross over somehow, from $\gamma_I = 1.75$ at $y = 1$ to $\gamma_G = 1$ at $y = 0$ (the latter value being off the range of γ shown on the plot). Such crossover behavior is certainly visible in Fig. 1. It may strike the reader as surprising that the variation of γ_{eff} is *nonmonotonic* in y , both the Kl and DG data attaining a maximum value of about 1.92 at which $y_{Kl} \approx 0.3$ and $y_{DG} \approx 0.5$, respectively. In fact, such nonmonotonic behavior has been seen in other contexts and can be calculated explicitly in $\epsilon = 4 - d$ expansions: see, for example, the figures presented by Seglar and Fisher³⁷ where one observes nonmonotonic overshoots of from 16% to 265%, as expressed by the fractions $|\gamma_{\text{eff}} - \gamma_A|_{\text{max}} / |\gamma_A - \gamma_B|$, in which γ_A and γ_B represent the known limiting values. In the present case the overshoot seen is about 23% in magnitude, which does not, thus, seem excessive. It should also be noted that a significant fraction of the approximants in the range where γ_{eff} is maximal are found to be defective (in the sense of having spurious singularities in or close to the

physical range of x); this again suggests that a crossover effect is being observed.

A parallel single-variable analysis may, of course, be performed for the $\lambda\varphi^4$ lattice models (for which double power series are not available). Indeed, Baker and Johnson^{27(a)} have reported such a study for a special *border* case $\lambda = \lambda_b$ corresponding, in (2.31), to $u_2 \equiv 0$. [For the DG model one sees from (2.32) that the analogous case would be $y_{DG} = \frac{1}{2}$.] Baker and Johnson (BJ) find values of γ_{eff} in the range 1.90 to 2.00 for the border model: these correspond well with the maximal estimates of γ_{eff} we find for $y_{DG} \approx 0.5$ and $y_{Kl} \approx 0.3$. Furthermore, using 21-term series³² (longer than employed by BJ) we have also made a single-variable analysis of the $\lambda\varphi^4$ border model on the square lattice: our estimates for γ_{eff} agree well with the BJ values. On the basis of these border-model results Baker and Johnson asserted, as mentioned in the Introduction, that the $\lambda\varphi^4$ model in two dimensions admits a new, non-Ising-like universality class characterized by $\gamma_b \approx 2.0$ (rather than $\gamma_I = 1.75$). We regard this claim as dubious but postpone a detailed discussion of the issues to Sec. VI. We stress here, however, that we have also studied the series *away* from the border value λ_b , obtaining estimates for $x_c(\lambda)$ and $\gamma_{\text{eff}}(\lambda)$. To compare these results with those for the DG and Kl models we identify values of λ with corresponding values of y_{DG} by equating the estimates of x_c found in the two models. (Since x_c can be determined with a precision of better than 1 in 10^3 even when the γ estimates are disperse, this procedure entails negligible ambiguity. Note also how closely the DG and Kl plots of x_c track one another in Fig. 1.) On this basis the border value, λ_b , corresponds to $y_{DG} \approx 0.652$ or $y_{Kl} \approx y_{DG}^2 \approx 0.425$ and the results for γ_{eff} vary as shown by the dotted lines in Fig. 1. The close numerical resemblance to the double-Gaussian and Klauder results is remarkable! Note that γ_{eff} drops quite rapidly to around 1.75 when λ rises above λ_b . On the other hand, the maximum in γ_{eff} is fairly broad and the border value, λ_b , does not stand out in any noticeable way. (However, the apparent convergence of the γ estimates is poorest for $\lambda \approx \lambda_b$, where, in a number of cases, it is necessary to add the residues from split D log Padé poles to obtain regular estimates for γ .) In summary, when appropriately compared, the behavior of γ_{eff} in the $\lambda\varphi^4$ model is not significantly different than in the DG and Kl models.

B. Partial-differential approximants

Since single-variable techniques cannot probe effectively the multicritical behavior of $\chi(x, y)$, we turn to the method of partial-differential approximants (PDAs). The theory of partial-differential approximants and some of their applications have been expounded in the literature.^{10-12, 38, 39} However, a brief recapitulation of their definition and most relevant properties is appropriate here.

A PDA provides a means of extrapolating the information embodied in the coefficients $f_{ii'}$ of a given double-power-series expansion,

$$f(x,y) = \sum_{i,i'} f_{ii'} x^i y^{i'}, \quad (3.1)$$

when not all the coefficients are known. One may, in particular, hope to extract reliable estimates for the multisingular properties of the function $f(x,y)$. A partial-differential approximant

$$F(x,y) \equiv [J/L; M, N | K]_{f(x,y)}$$

satisfies the *defining equation*

$$U_J(x,y) + P_L(x,y)F(x,y) = Q_M(x,y) \frac{\partial F}{\partial x} + R_N(x,y) \frac{\partial F}{\partial y}, \quad (3.2)$$

where U_J , P_L , Q_M , and R_N are polynomials in x and y , of the form

$$U_J(x,y) = \sum_{(j,j') \in J} u_{jj'} x^j y^{j'}, \quad (3.3)$$

specified by assigned label sets J , L , M , and N . When they are unimportant we will omit the label set subscripts. The polynomial coefficients $u_{jj'}$, $p_{ll'}$, $q_{mm'}$, and $r_{nn'}$ are found by matching the coefficients of $x^k y^{k'}$ on the left- and right-hand sides of (3.2) for all (k,k') in a specified matching set, K , when the known series for $f(x,y)$ is substituted for $F(x,y)$. This provides a set of linear algebraic equations, the *generating equations*, for the polynomial coefficients. Once the polynomials are known, the approximant $F(x,y)$ can be constructed by integrating (3.2) using appropriate boundary conditions [see Refs. 12 and 39(a)] specified on some boundary locus in the (x,y) plane on which $f(x,y)$ is known, or can be estimated reliably. In both theory and practice the integration of (3.2) is best accomplished by the method of characteristics. In the present case we have $x = 4J/k_B T$ and y is the crossover parameter in the KI and DG models.

Now for the Klauder model, rather than directly analyzing the series for the full susceptibility, $\chi_{KI}(x,y)$, we first study PDAs for the closely related function

$$f_{KI}(x,y) = \chi_{KI}(x,y) - 1. \quad (3.4)$$

The point of this is that the series expansion for f_{KI} is *upper triangular* (i.e., $f_{ii'} = 0$ for all $i < i'$), and, in addition, has vanishing diagonal elements. It is then possible, following arguments developed in Ref. 39(a), to choose sets J , L , M , N , and K so as to ensure that the PDA satisfies $F_{ii'} = 0$ for all $i \leq i'$, i.e., is also upper triangular. On the other hand, the first coefficient on the diagonal of the expansion for $\chi_{KI}(x,y)$ is 1 and the desired vanishing of all the other elements on the diagonal for $F(x,y)$ cannot be ensured readily.

For the double-Gaussian model we choose to study the simple product

$$f_{DG}(x,y) = x \chi_{DG}(x,y), \quad (3.5)$$

since this is again upper triangular, whereas χ_{DG} is not.

We now discuss the constraints that may be imposed on the PDAs in order to ensure that they reproduce the

known behavior at the Gaussian limit $y=0$. [Here we follow the earlier work of Chen, Fisher, and Nickel,¹⁰ who studied the same problem for the $(d=3)$ -dimensional bcc series.] From (2.28) and the definition (3.4) we have

$$f_{KI}(x,0) = x/(1-x). \quad (3.6)$$

In order that the approximant, $F(x,0)$, share this exact property and preserve the upper triangular character of $f(x,y)$, we choose the defining polynomials U_J , P_L , Q_M , and R_N to be of the form¹⁰

$$U_J(x,y) = x^2 y \bar{U}(x,y), \quad (3.7)$$

$$P_L(x,y) = p^0(x) + xy \bar{P}(x,y), \quad (3.8)$$

$$Q_M(x,y) = x(1-x)p^0(x) + x^2 y \bar{Q}(x,y), \quad (3.9)$$

$$R_N(x,y) = y \bar{R}(x,y), \quad (3.10)$$

where \bar{U} , \bar{P} , \bar{Q} , and \bar{R} are upper triangular polynomials in x and y , and $p^0(x)$ is a polynomial in x alone. It is readily verified by substituting in (3.2), setting $y=0$, and using the boundary condition $F(x,0)/x \rightarrow 1$ as $x \rightarrow 0$ that (3.6) is reproduced.

One may, in addition, impose further constraints obtained by taking first derivatives with respect to y at the Gaussian limit. Thus from (2.28) we also obtain

$$\left[\frac{\partial f_{KI}}{\partial y} \right]_{y=0} = \frac{-[I(x)-1]}{(1-x)^2 I(x)}, \quad (3.11)$$

which diverges as $x \rightarrow 1$. On substituting this result, (3.6), and (3.7)–(3.10) in (3.2), and matching the leading, $1/(1-x)^2$, and next-to-leading, $1/(1-x)^2 \ln(1-x)$, divergences as $x \rightarrow 1$, one obtains

$$\bar{Q}(1,0) = \bar{R}(1,0) + p^0(1), \quad (3.12)$$

$$p^0(1) + \bar{R}(1,0) = 0. \quad (3.13)$$

These equations represent linear constraints on the polynomial coefficients, and thus, in calculating approximants, they may be imposed by adjoining the corresponding extra equations to the set of generating equations. (Of course, the relative sizes of the label and matching sets must be adjusted accordingly.)

For the double-Gaussian model, we choose U_J , P_L , Q_M , and R_N so as to reproduce the correct behavior of $f_{DG}(x,y)$ defined in (3.5), on and near the pure Gaussian axis $y=0$. Now the leading deviation is of order y^2 , and thus we choose¹⁰

$$U(x,y) = x^2 y^2 \bar{U}(x,y), \quad (3.14)$$

$$P(x,y) = p^0(x) + xyp^1(x) + x^2 y^2 \bar{P}(x,y), \quad (3.15)$$

$$Q(x,y) = x(1-x)[p^0(x) + xyp^1(x)] + x^3 y^2 \bar{Q}(x,y), \quad (3.16)$$

$$R(x,y) = y \bar{R}(x,y). \quad (3.17)$$

Here $p^0(x)$ and $p^1(x)$ are polynomials in x and, as with the Klauder model, \bar{U} , \bar{P} , \bar{Q} , and \bar{R} are upper triangular polynomials in x and y . Further, in order y^2 , we can match the leading, $\ln(1-x)/(1-x)^2$, and next-to-leading, $1/(1-x)^2$, divergent amplitudes that follow from (2.18) and (3.5). This results in the linear constraints

$$2\bar{R}(1,0)+p^0(1)=0, \quad (3.18)$$

$$\pi\bar{Q}(1,0)=p^0(1), \quad (3.19)$$

which can also be accommodated in constructing approximants.

We have studied about 180 PDAs for the Klaunder model which incorporate the Gaussian axis constraints (3.7)–(3.10); about half of these also satisfy the constraint (3.12) or both (3.12) and (3.13). For the double-Gaussian model, 120 PDAs have been studied with the $y=0$ constraints (3.14)–(3.17) imposed, and in about a sixth of these the $O(y^2)$ constraint (3.18) was also imposed.

Each approximant calculated corresponds to a distinct choice of the polynomial label sets J, L, M, and N and/or of the matching set, K. Important guidance in the optimal choice of label sets is provided by theorems on *faithfulness* [meaning that $F(x,y)$ should reproduce all those exact expansion coefficients of $f(x,y)$ that are used in its construction] and on *Euler invariance*. This latter property, the analog of the well-known feature for ordinary Padé approximants, means that the approximant $\bar{F}(x,y)$ generated from $f(x,y)$ by first making the Euler transformation $x \Rightarrow \bar{x} = Ax/(1+Bx)$ (for any $A \neq 0$ and B) should, on inverting the transformation, be identical with the original approximant, $F(x,y)$, computed directly. Euler invariant approximants should be more accurate and reliable since they are independent of the particular location of the singularities of $f(x,y)$ in the complex x plane. Theorem 6.3 of Ref. 39(b) specifies precisely conditions which ensure Euler invariance. To indicate these we define a label set $J \equiv \{(j,j')\}$ to be *flush right* if each row in the corresponding Cartesian array has a gapless sequence of elements running downwards from (\hat{j},j') as $(\hat{j}-1,j')$, $(\hat{j}-2,j')$, . . . , to $(j_{\min}(j'),j')$ where \hat{j} is the same for all rows and, hence, represents the largest power of x in $U_j(x,y)$; however, the lower limit $j_{\min}(j')$ may depend on j' and may even exceed \hat{j} , specifying an *empty* row. If, in direct analogy to \hat{j} , the largest powers of x in the flush-right arrays L, M, and N are \hat{l} , \hat{m} , and \hat{n} , respectively, a necessary condition for Euler invariance (on x) is

$$\hat{j} = \hat{l} = \hat{m} - 2 = \hat{n}. \quad (3.20)$$

In addition, for upper triangular functions, J and L must be contained in upper triangular arrays, while M and N must be contained in upper triangular arrays which have been diminished or augmented, respectively, by one diagonal: compare with (3.7)–(3.10), (3.14)–(3.17), and see Theorem 6.3 of Ref. 39(b). The matching set K should be upper triangular and *flush left*.

In our work we computed a selection of fully Eulerian approximants of high order. In addition, however, we studied near-Eulerian approximants which should also be reasonably reliable. Specifically, we chose label sets J, L, M, and N corresponding to full or almost full upper triangular arrays (augmented or diminished by diagonals as indicated above), with zero, one, or two missing elements in the last column. A single such “vacancy” was usually placed at the bottom of the last column (consistent with Eulerian invariance), but some approximants were tried in

which the vacancy was placed on the top row. The limits \hat{l} , \hat{m} , and \hat{n} were selected in accordance with (3.20) or with deviations of magnitude at most unity. However, the label sets J were normally taken smaller than L, M, and N, with \hat{j} ranging between 0 and 3 for $\hat{l}=9$ or 10. This spoils precise Eulerian invariance [although a *homogeneous* PDA with $J \equiv \emptyset$, i.e., $U(x,y) \equiv 0$ can be Euler invariant]; it was judged, however, to be better to allow larger arrays M and N, in particular, since these determine the *flow patterns* of the trajectories of characteristics of (3.2) and thence, as we will explain, the critical locus. The polynomial $U_j(x,y)$, on the other hand, mainly determines the “background” near criticality,¹² which, for strongly divergent functions like the ferromagnetic susceptibility, should not normally be so important. [Note also the result of Ref. 39(b) about the covariance of the multicritical estimates under the addition to $\chi(x,y)$ of some lower-order polynomial $C_H(x,y)$.]

C. PDA flow patterns

As mentioned, the most appropriate method of solving the defining partial-differential equation (3.2) is by integration along the characteristics. These may be constructed by defining a timelike variable τ and solving the ordinary differential equations

$$\frac{dx}{d\tau} = Q(x,y), \quad \frac{dy}{d\tau} = R(x,y). \quad (3.21)$$

A solution of these with given initial conditions specifies a definite *trajectory* in the (x,y) plane. The set of all trajectories defines a flow pattern which is characteristic of the approximant in question. The flow pattern for a typical approximant is illustrated in Fig. 2.

One easily sees that the trajectories do not meet or cross except at the *multisingular points* of the approximant which are determined by the *fixed-point* equations

$$Q(x,y) = R(x,y) = 0, \quad (3.22)$$

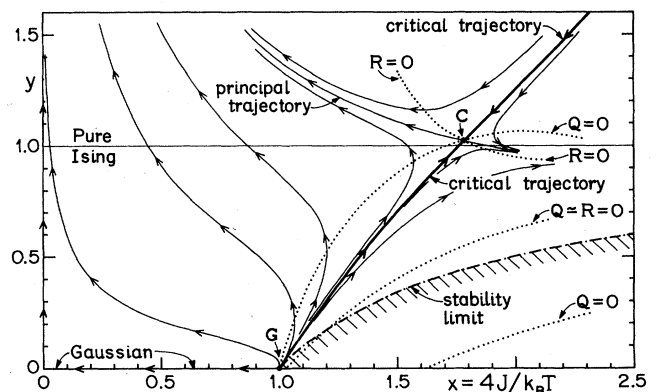


FIG. 2. A characteristic flow pattern of PDA trajectories. This example is for the Klaunder model with the Gaussian fixed point G at $(x,y)=(1,0)$, imposed. The Ising-like multicritical point C was located by the PDA through the intersection of the $R=0$ and $Q=0$ loci (shown dotted). This flow pattern implies that the critical behavior is Ising-like along the whole critical line from G through C (excluding G itself).

i.e., by the joint zeros of Q and R . The loci of zeros are shown by dotted curves in Fig. 2. Because the slope, dy/dx , of a trajectory passes through zero and changes sign when it crosses an $R=0$ locus, whereas the slope passes through infinity (and changes sign) when a trajectory crosses a $Q=0$ locus, the arrangement of zero loci determines the overall topology of the flow pattern. When, as in the example shown in Fig. 2, the Gaussian multicritical point G is imposed, one multisingular point lies *precisely* at G . Another is expected to represent a multicritical point C of Ising-like character as gauged by, say, an estimated exponent γ close to $\gamma_I \equiv 1.75$. In Fig. 2 this multisingularity occurs near the pure Ising line $y=1$ and has $\gamma \simeq 1.7427$. The trajectory leading from G to C must now be a line of singularities in the approximant and, hence, it represents the expected critical locus, $x_c(y)$, of, in this instance, the Klauder model. The flow pattern of Fig. 2 implies that the critical behavior all along this critical locus is Ising-like (except right at the Gaussian point at $y=0$) with the same exponent γ as at C . The scaling behavior near C contrasts with the normal crossover or bicritical situation^{11,12} in that the *crossover exponent*, ϕ , is *negative* here and governs only *corrections to scaling*. However, with $\phi \equiv -\theta$ the analogous scaling form^{10,12} holds in that, close to C , the approximant verifies

$$F(x,y) \approx \bar{t}^{-\gamma} Z(\bar{y}\bar{t}^\theta) + B_0 + \dots, \quad (3.23)$$

where \bar{t} and \bar{y} denote the *linear scaling fields* which are given by

$$\bar{t} = (x_c - x) - (y_c - y)/e_2, \quad (3.24)$$

$$\bar{y} = (y_c - y) - e_1(x_c - x). \quad (3.25)$$

The appropriate slopes, e_1 and e_2 , of the \bar{t} (or $\bar{y}=0$) axis and of the \bar{y} (or $\bar{t}=0$) axis, respectively, and the exponents γ and θ , are found by linearizing the PDA polynomials about C : the required explicit formulas are given in Refs. 12 and 40. Thus for the approximant of Fig. 2 one obtains $\theta \simeq 1.3729$ and $e_1 \simeq 0.2598$, $e_2 \simeq 1.0858$. Note that e_2 must also represent the *slope of the critical locus* at C .

In order to determine the *scaling function*, $Z(z)$ in (3.23), the approximant $F(x,y)$ must be evaluated by integration. When reexpressed using (3.21), the PDA-defining equation (3.2) leads to an equation of motion for F , namely^{12,39}

$$\frac{dF}{d\tau} = U(x,y) + P(x,y)F, \quad (3.26)$$

in which $x=x(\tau)$ and $y=y(\tau)$ are found by integrating (3.21) along a particular trajectory (on which only τ changes). In order to determine $F(x,y)$ in a region in the (x,y) plane, one needs initial conditions for $F(x,y)$ along some boundary locus which cuts across those trajectories which lead into (or out from) the region of interest. For instance, for the trajectory flow pattern shown in Fig. 2, any boundary locus that intersects the *principal trajectory* (leading out from C —see the figure), even if far from the multicritical region near C , suffices to determine $F(x,y)$ close to C and thereby the scaling function $Z(z)$.¹² In practice, one might take a boundary locus at, say, $x=0.5 \equiv \frac{1}{2}x_G$ on which $f(x,y)$ can be calculated accu-

rately by direct Padé approximants or, even, merely by summing the truncated series (since $2^{-21} < 10^{-6}$). For most qualitative purposes, however, it is sufficient to know only that $F(x,y)$ and all its derivatives exist and define F on the boundary locus. Indeed, this is enough to conclude, in general,^{1,40} that $Z(z)$ has an expansion

$$Z(z) = Z_0 + Z_1 z + \dots \quad (3.27)$$

From this it follows that θ is the leading correction-to-scaling exponent which enters asymptotic expressions as in (1.1). Furthermore, this same exponent must, like γ , apply along all sections of a critical line which are represented by trajectories flowing into C .

Now, when one computes a variety of approximants (with differing polynomial shapes and orders) one finds that not all approximants display flow patterns similar to that in Fig. 2. Examples of other types found in our study are sketched in Figs. 3 and 4. The flow patterns shown in Fig. 3 are similar to that in Fig. 2 in that there are no extra fixed points on the critical locus between G and C . It follows, just as for Fig. 2, that the critical behavior implied by these approximants is Ising-like all along GC (for $y > 0$). Once again, the scaling function $Z(z)$ describing the behavior near the critical locus can be determined explicitly if boundary conditions are specified on a locus that intersects the principal trajectory transversely. The extra fixed point, D , is found on the Gauss-

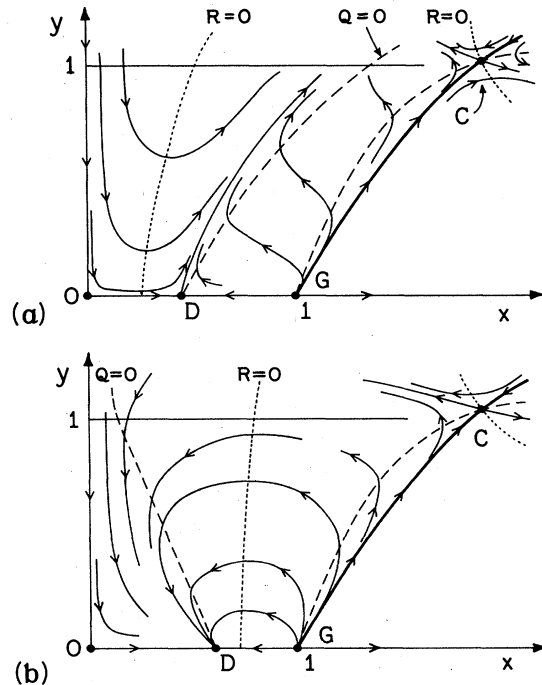


FIG. 3. Schematic examples of other flow patterns found in some approximants. Like the pattern in Fig. 2, Ising-like critical behavior prevails between G and C . The dashed and dotted curves are loci of $Q=0$ and $R=0$, respectively.

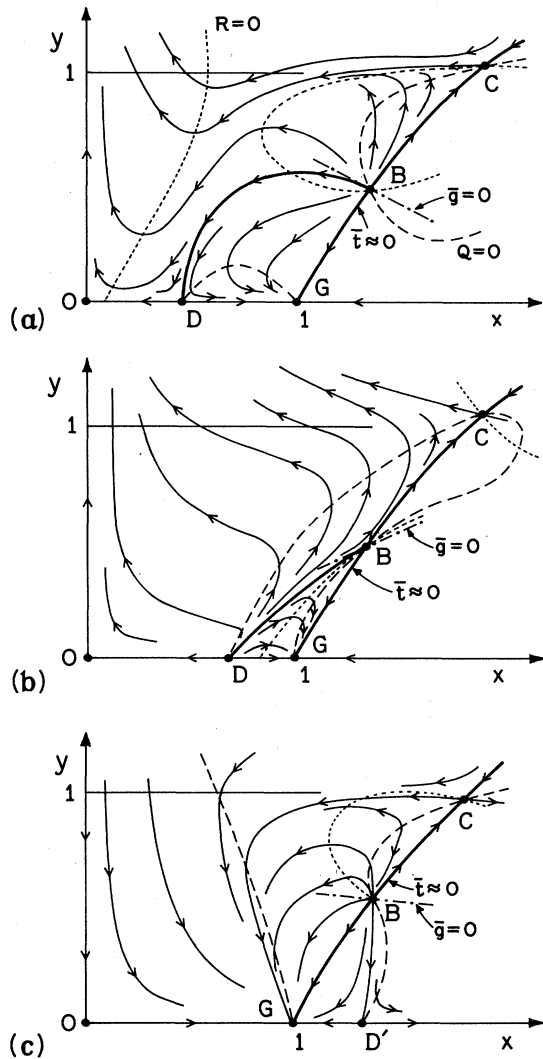


FIG. 4. Schematic flow patterns which display an extra fixed point B in the vicinity of the critical locus. The loci BD in (a) and (b) are, in general, singular, but as discussed in Appendix B, the singularity may be removed in case (a) by choosing the boundary locus to cut BD , along, say, a path parallel to the x axis. In practice, the fixed point D in (b) is actually found very close to G , with $x_D > 0.95$: the separation has been increased in the figure for clarity.

ian axis. It can reasonably be regarded as a *defect*¹² (hence the chosen label) since it occurs in a region of the (x, y) plane ($x < x_G$) where one has excellent reasons to believe (and might even be able to prove rigorously) that the underlying function, $f(x, y)$ [or $\chi(x, y)$], is analytic in both x and y . The analogous phenomenon of *defective* or *spurious* poles is well known in applications of ordinary, single-variable Padé-approximant techniques: the reasons for its occurrence, however, are currently rather obscure although some light has recently been cast on the problem by Nuttall.⁴¹ For the reasons given we ascribe no physical significance to D or to the associated exponents γ_D

[which vanishes identically as a result of the imposed Gaussian value of $F(x, y)$ for $y = 0$; see Appendix B] and ϕ_D (which is found to range from $+0.70$ to -0.61).

In contrast to Figs. 2 and 3, the flow patterns in Fig. 4 exhibit an additional intermediate fixed point, labeled B , on the trajectories linking G to C . This has the important consequence of changing the critical behavior along the locus GC ; it is now Ising-like *only* from B up to (and through) C , whereas it is Gaussian in character (with $\gamma = \gamma_G \equiv 1$) along BG . The new critical exponent γ_B appropriate to B is typically in the range 1.1 to 2.0; see Figs. 5 and 6 below. (The significance of B is discussed further in Sec. VI.) In the majority of cases, B is totally unstable, with an ill-determined positive crossover exponent, ϕ_B , typically in the range 2.0 to 8.0. Roughly half of the approximants which display a fixed point of type B also exhibit another fixed point in the physical region, $x \leq x_C(y)$: most often there is just one extra fixed point, D , on the x axis, as illustrated in Figs. 4(a) and 4(b). As we explain in Appendix B, the segment DB will then, in general, also be singular, although, as indicated above, we expect that such an extra singular locus is quite spurious. In other cases, as illustrated in Fig. 4(c), there is a further fixed point near to but not in the physical domain.

All the flow patterns we have discussed exhibit hyperbolic flows around the Ising-like multicritical point C , i.e., $\theta_C > 0$. Not surprisingly (in view of the fact that B , when present, is quite far from C even though it is often close to G), the value of θ_C is relatively insensitive to the global nature of the flows. Nevertheless, we have distinguished between two types of approximants: type A denotes those approximants with $\theta_C > 0$, in which there is no extra fixed point on the critical trajectory GC (as illustrated in Figs. 2 and 3); type B denotes those approximants with $\theta_C > 0$ in which there is a multisingular point B on the locus GC as in Fig. 4. For the Klauder model, 156 of the 179 PDAs studied (i.e., 87%) display a stable Ising-like multicritical point (with $\theta_C > 0$); the remaining approximants either display no Ising-like fixed point in the region $y \leq 1.5$ or else, more rarely, have $\theta_C < 0$ (i.e., $\phi_C > 0$). Of the 156 with the expected, stable Ising-like multicritical point, 103 (i.e., two-thirds) are of type A . In the case of the double-Gaussian model, 76 of the 120 PDAs studied have $\theta_C > 0$, and of these 42 (i.e., 55%) are of type A . The reason for the more erratic behavior of the double-Gaussian model is not obvious, but the issue is commented on further in Sec. VI.

Besides PDAs in which the Gaussian axis constraints were imposed, we also studied 100 or more for both models in which a flow was instead imposed *along the Ising axis* ($y = 1$). The reason for considering such approximants is the strong suspicion, explained in the following section, that the *true* nonlinear Ising-like scaling axis coincides with $y = 1$. In practice, such a flow is most easily imposed by transforming the series by a translation to $g = 1 - y$ and then choosing $R(x, g)$ to have the form $g\bar{R}(x, g)$. We expect¹² such a PDA to approximate an ordinary Dlog Padé approximant along the Ising axis. Indeed, it reduces exactly to a Dlog Padé when the relation

$$\hat{l} + \hat{m} = \hat{k} + 1 \quad (3.28)$$

holds. In our studies, discrepancies as large as 2 or 3 between the left- and right-hand sides of this relation were allowed, with $\hat{k}=19$ or 20. We chose to study $\chi_{KI}(x,y)$ rather than $f_{KI}(x,y)$ as this choice yields better estimates for γ (see Sec. IV). As with the Gaussian-axis-constrained PDAs, the majority of approximants display hyperbolic flows around the Ising multicritical point (i.e., $\theta_C > 0$). However, it should be mentioned that approximants of this type often display spiral flows around a fixed point near $y=0$, i.e., the eigenvalues of the linearized trajectory equations around the corresponding fixed point become complex. Such behavior is, of course, quite unphysical but it does not seem to have a significant effect on the estimates for the Ising-like multicritical parameters.

In the same spirit we also considered the imposition of the exact Onsager value¹⁴ of $x_C = x_I \simeq 1.7627$ and the exact value of $\gamma_C = \gamma_I \equiv 1.75$ on approximants with Ising axis flows. The 60 or so approximants calculated for each model which were constrained in this way were rather disappointing. Quite often they displayed a second, spurious, Ising-like fixed point close to $y=1$: anomalous flow patterns, with correspondingly anomalous values of θ , then resulted.

Finally, we constructed a few dozen approximants in which almost all of the exactly known (or reasonably conjectured) properties of the susceptibility were imposed. This included the imposition of flows along *both* the Gaussian and the Ising axes and the requirements $x_C = x_I$ at $y=1$, and $\gamma_C = 1.75$. However, this class of approximants shared most of the defective properties of the x_C - and γ_C -constrained approximants without the Gaussian axis constraints. Overall, it seems that the most regular and physically reasonable flow patterns in the neighborhood of C are generated by approximants subject to the fewest constraints: The reason why this is so is not presently understood, but various tests and lines of argument¹² suggest that it is associated with the negative value of ϕ or, in other words, with the fact that only corrections to scaling are involved.

IV. ISING MULTICRITICALITY

In the preceding section we described the construction of partial-differential approximants and the interpretation of the implied multicritical behavior. The estimates for the significant multicritical parameters vary from one approximant to another. Of course, this feature also characterizes ordinary, single-variable Padé and Dlog Padé analysis.³⁵ In that case, however, it is feasible to calculate and display the entire Padé table in deriving overall estimates and assigning reasonable confidence limits. Unfortunately, the astronomical number of possible PDAs calculable even for series half the length of those available here,^{39(b)} makes the analogous approach quite unworkable. Instead, we rely on the judicious choice of approximants using the invariance criteria explained [see also Refs. 39(b) and 39(c)] and adopt a statistical outlook on the analysis and evaluation of the data resulting from the PDA calcu-

lations.^{10,11} Of course, all the computations with any given approximant are performed "exactly" in a numerical sense so there is no stochastic aspect *per se*; but one can only sample the population of all the possible approximants that one might, ideally, wish to examine. [Incidentally, various precautions were taken, including the use of quadruple precision, to test the oft-repeated inversions of 200×200 or larger matrices and so ensure that roundoff errors were insignificant at the relevant level of precision: Because of the scatter in the estimates, even in favorable cases, 1 part in 10^6 or 10^7 precision in the estimates of multisingular positions, (x_C, y_C) , and of about 1 part in 10^4 or 10^5 in exponent estimates, is quite adequate although most of our results are significantly better.]

We consider first those approximants in which a flow was imposed only along the Gaussian axis. As commonly observed in multiparameter analysis, there is a fairly pronounced correlation between estimates for various pairs of multicritical parameters. This is evident in Figs. 5 and 6, which are correlation plots of the estimates of the susceptibility exponent, γ , versus the corresponding multisingular ordinate y for the Ising-like multicritical point C , and, when it is present, for the multisingular point B . [It may

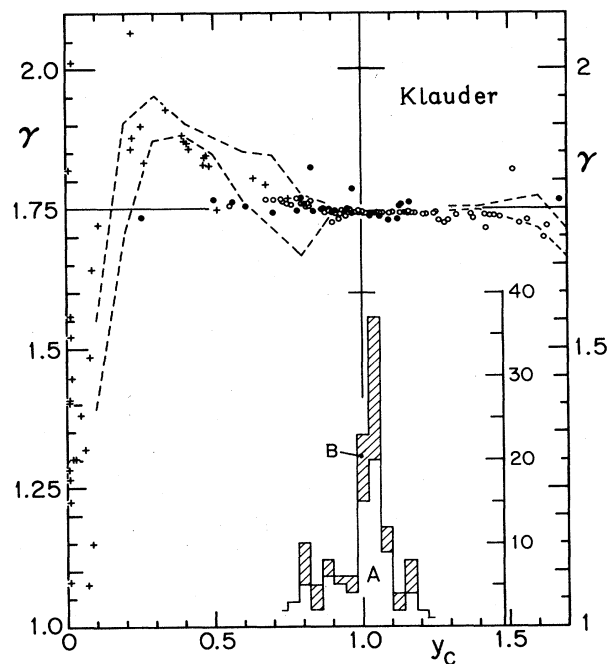


FIG. 5. Correlation plot for the susceptibility exponent estimates γ versus the y coordinate of the corresponding estimated multisingular point for the Klauder model. Data for both the Ising-like fixed point C (circles) and the border fixed point B (crosses) are included. The dashed lines recall the results of single-variable analysis (see Fig. 1). The histogram demonstrates the concentration of estimates for the ordinate of the Ising-like fixed point close to $y=1$: A and B denote approximants with the flow pattern of Figs. 2 and 3 and, respectively, with the flow patterns of Fig. 4, which exhibit the extra multisingularity, B .

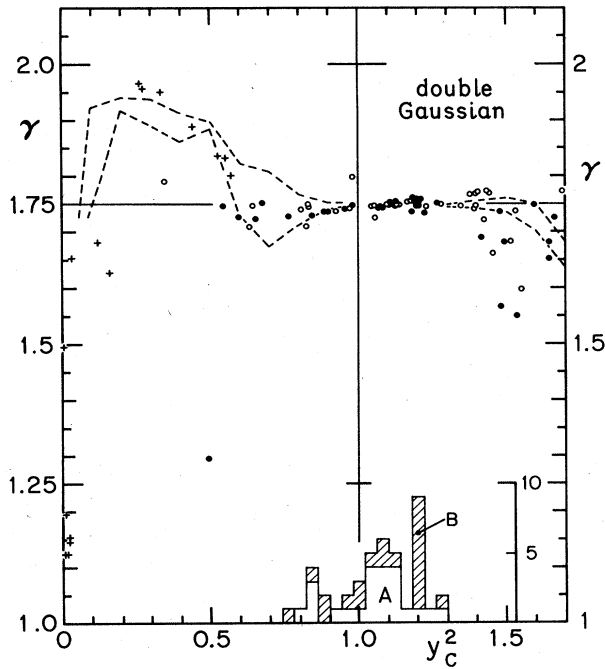


FIG. 6. Correlation plot of γ versus y as in Fig. 5, but for the double-Gaussian model.

be mentioned that the correlation between the multisingular parameters x_C and y_C is so close since, essentially, they lie on the critical locus $x_c(y)$, that no scatter from a smooth curve is visible in a graphical plot like Fig. 1.]

For both Klauder and double-Gaussian models the general trend of the combined C and B estimates for γ in Figs 5 and 6 tracks fairly closely the results of the single-variable analysis displayed in Fig. 1. Owing to the crowding of the data points it is not possible to display all the C estimates on the figures: Accordingly, the histograms in the lower part of each figure show (for $0.7 \leq y \leq 1.3$) the numbers of approximants yielding a value of y_C in a given interval. The estimates deriving from type- B approximants (with flow patterns like those in Fig. 4) have been shaded. Apart, perhaps, from an anomalous concentration of type- B approximants near $y_C = 1.2$ in the double-Gaussian model, the distributions obtained from type- A and $-B$ approximants do not differ significantly: neither do the γ estimates for which overall we would quote

$$\gamma_C(\text{Kl}) = 1.743 \pm 0.005, \quad \gamma_C(\text{DG}) = 1.745 \pm 0.007. \quad (4.1)$$

Both estimates deviate systematically below the exact Ising result $\gamma_I = 1.750$, but the accuracy is nevertheless quite gratifying in view of the fact that the approximants are quite unbiased as regards any Ising-like behavior.

It is also striking, especially for the Klauder model, that the y_C estimates cluster strongly around the pure Ising value $y = 1$. This is in contrast to the situation in $d = 3$ dimensions¹⁰ where the PDAs locate a clear Ising-like multicritical point in the vicinity of $y_C(\text{Kl}) \approx y_C^2(\text{DG}) \approx 0.81 < 1$. Although direct averages of the data for $d = 2$ might suggest $y_C(\text{Kl}) = 1.01 \pm 0.03$ and

$y_C(\text{DG}) = 1.03 \pm 0.05$, it is natural to conjecture that the exact location of the Ising-like multicritical point, C , for both models lies on the pure Ising axis, i.e., $y_C = 1$. Further independent support for this conclusion follows from theoretical conclusions concerning perturbations about the Ising limit that are described in the next section.

If one accepts $y_C = 1$, as we will henceforth, it follows from the identity of the Kl and DG models to first order in $g = 1 - y$ (discussed in Sec. II) that the slope $e_2(\text{Kl})$ of the $\bar{t} = 0$ scaling axis should be exactly twice the corresponding slope, $e_2(\text{DG})$, for the double-Gaussian model. Further, as explained, e_2 should then be the slope of the critical locus, $x_c(y)$ at $y = 1$. Figure 7 displays the observed correlation between the e_2 estimates and the ordinate y_C : Although there is a paucity of DG approximants with y_C close to 1.00, the two plots agree closely in the vicinity and we estimate

$$e_2(\text{Kl}) \equiv 2e_2(\text{DG}) = 1.091 \pm 0.003. \quad (4.2)$$

The estimates for the slopes, e_1 , of the other scaling axis (the thermal axis, $\bar{y} = 0$) at C are relatively small and of opposite signs in the two models if $y_C = 1$ is accepted. The data suggest

$$e_1(\text{Kl}) = -0.25 \pm 0.15 \quad \text{and} \quad e_1(\text{DG}) = 0.05 \pm 0.10. \quad (4.3)$$

However, in view of the identity of the two models to first order in $g = 1 - y$, we are strongly inclined to believe that there are systematic effects [probably associated with the choice (3.4)] which cause the Klauder estimate to be negative and unequal to the DG estimate. The latter slope vanishes to within the available precision (which is, perhaps, disappointingly low, but see below). Thus we actually believe that the thermal axis slope e_1 , should be

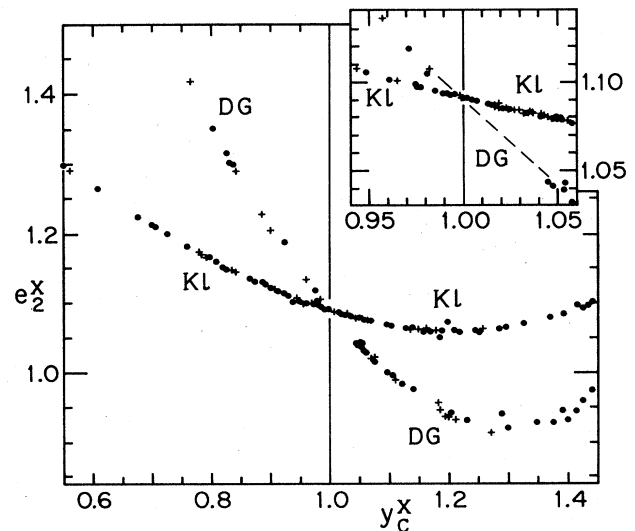


FIG. 7. Correlation between the slope of the critical curve and the ordinate at the multicritical point C . For the Klauder model e_2^x and y_C^x denote $e_2(\text{Kl})$ and $y_C(\text{Kl})$, respectively; for the double-Gaussian model they denote $2e_2(\text{DG})$ and $y_C^2(\text{DG})$. The dots and crosses distinguish type- A and $-B$ approximants, respectively.

identically zero in both models. As in the conclusion $y_C \equiv 1$, the theoretical analysis of perturbation theory about the pure Ising model provides independent support for this belief.

Finally, we consider the main object of our inquiry, namely the *correction-to-scaling exponent* θ at the Ising-like multisingularity. It is clear from the plots versus y_C in Figs. 8 and 9 that there is considerable scatter in the θ estimates for both models, although, as for the other multicritical parameters, the Klauder model displays more uniform behavior. The weight of evidence, however, clearly indicates $\theta > 1$. This implies a singular correction that is very small in numerical terms, less, indeed, than the first analytic term: By contrast, we have $\theta \simeq 0.54$ for $d=3$ and the singular corrections dominate. The small size of the correction in absolute terms would seem to be the reason for the fairly broad scatter in the estimates of y_C and of the axis slope e_1 , as well as of θ itself. If we accept $y_C=1$ and include only approximants with $y_C(\text{K1})$ and $y_C^2(\text{DG})$ in the range (0.85,1.15), we would estimate $\theta(\text{K1})=1.38 \pm 0.25$ and $\theta(\text{DG})=1.25 \pm 0.26$.

On the other hand, if we accept $y_C=1$, it is appropriate to examine approximants with a flow forced along the pure Ising axis and the dispersions then diminish. Histograms of the θ estimates for such approximants (shaded) and for the original Gaussian-flow approximants are displayed in Fig. 10. For the former we find $\theta(\text{K1})=1.27 \pm 0.27$ and $\theta(\text{DG})=1.30 \pm 0.38$. While each set of approximants almost surely suffers from certain systematic errors, the collective evidence seems to point to a value of θ between 1.2 and 1.5: Our overall estimate is

$$\theta = 1.35 \pm 0.25. \quad (4.4)$$

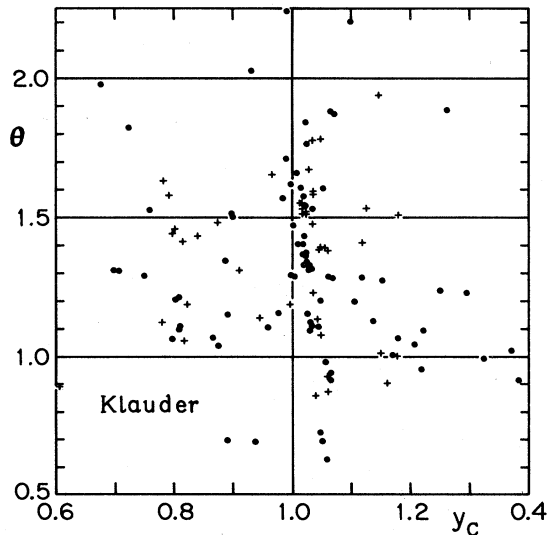


FIG. 8. Estimates for the Ising-like correction exponent, θ , versus the multicritical ordinate, y_C , for the Klauder model. The dots and crosses denote type-*A* and -*B* approximants, respectively.

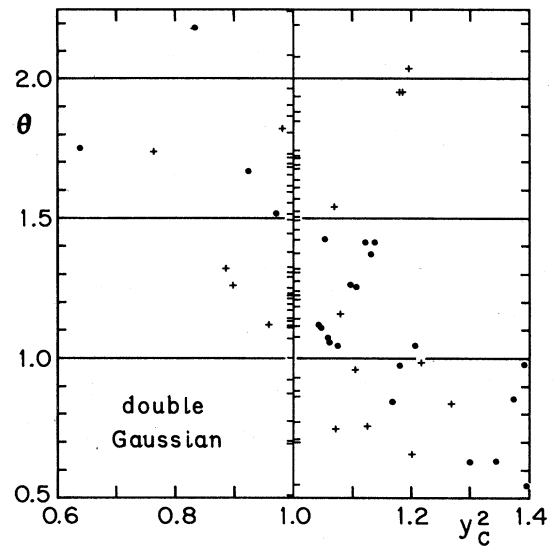


FIG. 9. Plot of the correction exponent estimates for the double-Gaussian model as in Fig. 8, but with results for approximants in which an Ising axis flow is imposed indicated on the $y=1$ axis.

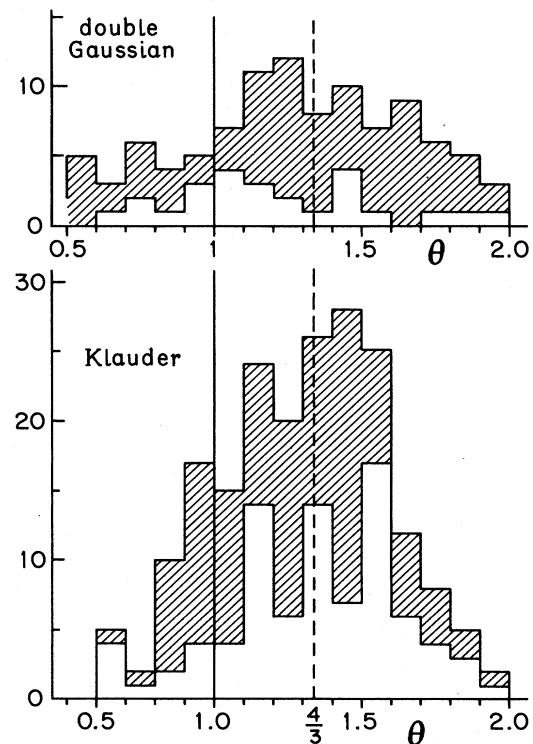


FIG. 10. Histograms of the correction exponent θ at the Ising multisingular point. The shading indicates PDA with a flow imposed along the pure Ising axis; the remaining approximants have only Gaussian axis flows imposed and y_C restricted to the range 0.85 to 1.15.

Notice that Nienhuis's value $\theta = \frac{4}{3}$ is clearly consistent with our estimates!

While imposing a flow along the Ising axis does not affect the estimates of the correction exponent θ very much, there is a more pronounced effect on the estimate of the leading exponent γ ; this improves to $\gamma_C = 1.7485 \pm 0.0015$ for the Klauder model, and to 1.7495 ± 0.0015 for the double-Gaussian model, both very close to $\gamma_I = 1.7500$. If, further, x_C is constrained to the exact Onsager value,¹⁴ there is a further improvement to $\gamma_C \simeq 1.7499 \pm 0.0003$ for both models. Recall, however, that despite this improvement in the estimates for γ , anomalous flow patterns, with correspondingly erratic estimates of θ , are characteristic of this last class of approximants. Overall, however, we find that the estimates of θ_C are not affected a great deal by the global flow pattern so long as other fixed points (even if spurious) are some distance away from the multicritical point of interest, C .

V. SCALING AROUND THE ISING MULTISINGULARITY

As demonstrated in the preceding section, our PDA analysis of the Klauder and double-Gaussian models is consistent with the following assertions: (i) the Ising-like multicritical point in both ($d=2$)-dimensional models coincides with the critical point of the pure Ising model (in contrast to the situation for $d=3$); (ii) the pure Ising axis $y=1$ is the principal (or thermal) linear scaling axis; (iii) the (apparent) correction exponent θ has the value $\frac{4}{3}$, in accord with Nienhuis's conjecture;¹⁸ see (4.4). In this section we discuss the implications of these three assertions for the scaling behavior of the susceptibility in the neighborhood of the multicritical point. In the light of exact knowledge about the pure Ising model, we will uncover a paradoxical situation: a resolution is proposed based on a detailed property of the *nonlinear scaling fields*,¹ which can be tested by means of further calculations for the Ising model.

A. Scaling fields

Consider first the *linear* scaling fields introduced generally in (3.24) and (3.25). It follows from (i) and (ii) that these must be

$$\bar{t} = t - g/e_2 \quad \text{and} \quad \bar{g} = g \equiv 1 - y, \quad (5.1)$$

where, in terms of $T_{c,I}$, the exact pure Ising critical point,¹⁴ we have

$$t = x_I - x \quad \text{with} \quad x_I = 4J/k_B T_{c,I}. \quad (5.2)$$

[The value of e_2 is known numerically through (4.2) but will play only an insignificant role.] Now the nonlinear scaling fields introduced originally by Wegner,¹ say $\tilde{t}(t, g)$ and $\tilde{g}(t, g)$, are defined in terms of the renormalization-group flow equations for \bar{t} and \bar{g} (or for t and g). For small t and g , i.e., near the multicritical point, the nonlinear fields reduce to \bar{t} and \bar{g} . In terms of them one may anticipate that the standard scaling form

$$\chi(T, y) \approx C \bar{t}^{-\gamma} Z(\bar{g} \bar{t}^{-\theta}), \quad (5.3)$$

with, here, $\theta = \frac{4}{3}$, provides a valid asymptotic description of the singular behavior of the susceptibility.¹ Note that inclusion of the amplitude C allows one to require that the scaling function $Z(z)$ satisfies the normalization condition $Z(0) = 1$.

If one neglects other irrelevant scaling fields the renormalization-group flow equations for t and $g \equiv \bar{g}$ may be written¹

$$\frac{d\bar{t}}{dl} = \lambda_1 \bar{t} + B_{1,1}^t \bar{t}^2 + B_{1,2}^t \bar{t}g + B_{2,2}^t g^2 + \dots, \quad (5.4)$$

$$\frac{d\bar{g}}{dl} = \lambda_2 \bar{g} + B_{1,1}^g \bar{t}^2 + B_{1,2}^g \bar{t}g + B_{2,2}^g g^2 + \dots, \quad (5.5)$$

where l is the standard flow parameter that describes the rescaling of spatial dimensions by the factor e^l . The coefficients $\lambda_1 \equiv \lambda_t = 1/\nu$ and λ_2 are the renormalization-group eigenvalues associated with \bar{t} and g : For the two-dimensional Ising model the correlation-length exponent is simply^{13,14} $\nu = 1$. The correction exponent is then given generally by

$$\theta = -\lambda_2/\lambda_1. \quad (5.6)$$

By solving (5.4) and (5.5) iteratively,¹ one constructs the nonlinear scaling fields as formal power series in \bar{t} and g which satisfy the canonical flow equations

$$\frac{d\tilde{t}}{dl} = \lambda_1 \tilde{t} \quad \text{and} \quad \frac{d\tilde{g}}{dl} = \lambda_2 \tilde{g}, \quad (5.7)$$

which have obvious solutions. When this procedure goes smoothly, \tilde{t} and \tilde{g} appear as infinitely differentiable (i.e., C_∞) functions of \bar{t} and g .

Without deriving and solving (5.7), however, certain quite definite conclusions may be reached on the basis of (5.3). First recall, as discussed in the Introduction, that the exact work on the pure Ising model^{13-15,19} reveals *no* correction terms in the susceptibility χ [see (1.1)] of the form $t^{j+1/3}$ and $t^{j+2/3}$ (with j integral) which one would expect on the basis of (5.3) with $\theta = \frac{4}{3}$ if \tilde{g} contained additive terms like t^2 , or t^4 , or t^5 , etc. Conversely, if one has

$$\tilde{g} = g[1 + o(g, t)], \quad (5.8)$$

such terms would automatically vanish on the Ising axis $g=0$ ($y \equiv 1$). This relation means that the *full* nonlinear scaling axis, $\tilde{g}=0$, *coincides* with the pure Ising axis!

One may, however, go further and examine the g dependence of the susceptibility at the Ising limit. In particular, in Sec. II we saw how $\chi(T, g)$ for both KI and DG models could be expressed to first order in g in terms of even-order spin-correlation functions like $\langle s(\mathbf{0})_s(\mathbf{R})_s(\mathbf{R}'') \rangle$ for the pure ($g=0$) Ising model. By performing similar calculations to higher order in g [which is particularly straightforward for the DG model in view of (2.20)], higher-order derivatives $(\partial^k \chi / \partial g^k)_{g=0}$ ($k=1, 2, \dots$) can equally be expressed as spatial sums over the pure Ising correlation functions. On the other hand, the singular behavior of such derivatives can also be obtained from the scaling form (5.3). Specifically, the scaling function should have an expansion

$$Z(z) = 1 + Z_1 z + Z_2 z^2 + \dots, \quad (5.9)$$

which implies that $(\partial^k \chi / \partial g^k)_{g=0}$ should contain additive singular terms of the form

$$Z_k t^{-\gamma+4k/3} \text{ for } k=1,2,\dots \quad (5.10)$$

(Note that other, more dominant singularities arise from the g dependence of the nonlinear field \tilde{t} which enters even in the linear field \bar{t} .) Now the critical-point decay laws for the pure Ising correlation functions are rather well understood;^{42,19,13} in particular, one concludes, as for $\chi(T,g=0)$ itself, that there can be no terms like (5.10) with $k=1,2,4,5,7,8,\dots$. This observation would be accounted for, however, if the scaling function were such that all its expansion coefficients Z_k vanish except for $k=3j=0,3,6,\dots$. Equivalently, one may suppose that $Z(z)$ is a C_∞ function only of the combination

$$z^3 \equiv w = \tilde{g}^3 \tilde{t}^4. \quad (5.11)$$

Now suppose that the nonlinear scaling fields \tilde{g} and \tilde{t} are C_∞ functions of \bar{g} and \bar{t} , as is generally true;¹ then the statement that Z has an expansion only in w would force us to conclude that the nature of the singularity in $\chi(T,g)$ at fixed g is the same away from $g=0$ ($y=1$) as at $g=0$. In other words, the critical point at $g=0$ ($y=1$) would not actually be multisingular in character. In view of the fact that the majority of PDAs rather clearly pick out a distinct, Ising-like multisingular point in the vicinity of $y=1$, this is clearly a paradoxical situation!

To escape this paradox we must identify some way in which $g=0$ is selected as a special multisingular point of $\chi(T,g)$, apparently characterized by a correction exponent $\theta = \frac{4}{3}$, while, at the same time, accounting for the fact that no correction terms involving the factors $t^{1/3}$ and $t^{2/3}$ appear in χ or any of its g (or t) derivatives at $g=0$. To this end we examine the flow equations (5.4) and (5.5) in more detail, following the elegant and seminal analysis of Wegner.¹

The crucial observation¹ on which we focus²⁶ is that the formal construction of the nonlinear scaling fields in powers of \bar{t} and g runs into difficulties if a vanishing denominator occurs in the expressions for the expansion coefficients. This in turn will occur if the resonance condition

$$k_1 \lambda_1 + k_2 \lambda_2 = 0 \quad (5.12)$$

is satisfied for some positive integers k_1 and k_2 . Since, by (5.6), λ_1 and λ_2 are of opposite sign (θ being taken positive), this merely means that λ_1 and λ_2 are *rationally related*, which, in turn, is certainly true if the correction exponent θ is rational—as expected here! Wegner¹ shows that when a resonance such as (5.12) (or, more generally, involving any other relevant or irrelevant eigenvalue, λ_r) occurs, one must anticipate the appearance of *logarithmic* factors in the expressions for \tilde{t} and \tilde{g} in terms of \bar{t} and \bar{g} .

B. Model renormalization-group flows

To see what is involved more explicitly and to discover what might arise in the Ising model, we will explore the simplest situation. Thus suppose that the nonlinear scaling fields \tilde{t} and \tilde{g} have been constructed without en-

countering any resonance phenomena up to order k_1+k_2 , where k_1 and k_2 are the smallest integers satisfying

$$\theta (= -\lambda_2/\lambda_1) = k_1/k_2. \quad (5.13)$$

Correct to this order we suppose that $\tilde{t} \approx \hat{t}$ and $\tilde{g} \approx \hat{g}$, where \hat{t} and \hat{g} are thus polynomials in \bar{t} and \bar{g} behaving as \bar{t} and \bar{g} when $t, g \rightarrow 0$. The flow equations may now be rewritten in terms of \hat{t} and \hat{g} in the form

$$\frac{d\hat{t}}{dl} = \hat{t}(\lambda_1 + D_1 \hat{t}^{k_1} \hat{g}^{k_2}), \quad (5.14)$$

$$\frac{d\hat{g}}{dl} = \hat{g}(\lambda_2 + D_2 \hat{t}^{k_1} \hat{g}^{k_2}), \quad (5.15)$$

where we have, for the sake of obtaining explicit closed-form answers, dropped (or absorbed into \hat{t} and \hat{g}) other, *nonresonant* terms of order k_1+k_2+1 as well as higher-order terms (which would, in general, also entail higher-order resonances): all lower-order terms have been accounted for¹ in the construction of \hat{t} and \hat{g} .

The solutions of these model flow equations are

$$\hat{t}(l) = \hat{t}_0 e^{\lambda_1 l} / (1 - D w_0 l)^{\mu_1}, \quad (5.16)$$

$$\hat{g}(l) = \hat{g}_0 e^{\lambda_2 l} / (1 - D w_0 l)^{\mu_2} \quad (5.17)$$

(see Appendix C), where \hat{t}_0 and \hat{g}_0 represent the initial ($l=0$) values, while

$$D = k_1 D_1 + k_2 D_2, \quad (5.18)$$

$$\mu_1 = D_1/D, \quad \mu_2 = D_2/D, \quad (5.19)$$

and we have written

$$w_0 = \hat{t}_0^{k_1} \hat{g}_0^{k_2}. \quad (5.20)$$

Now the l dependence in the denominators in (5.16) and (5.17) generates a logarithmic dependence of a thermodynamic variable, say $G(t,g)$, on \hat{t} and \hat{g} (and thence on \bar{t} and \bar{g}). In order to see this explicitly, suppose for simplicity that G undergoes only a constant multiplicative renormalization according to

$$\frac{dG}{dl} = \lambda_0 G, \quad (5.21)$$

which implies

$$G(\hat{t}_0, \hat{g}_0) = e^{-\lambda_0 l^\dagger} G^\dagger, \quad (5.22)$$

where G^\dagger is a noncritical reference, or matching value of G . On substituting for e^{l^\dagger} from (C15) in Appendix C and dropping the subscripts 0 (and replacing the circumflexes omitted in the Appendix), we find

$$G(\hat{t}, \hat{g}) \approx C_G \hat{t}^{-\gamma} [\mathcal{L}(\hat{t}, \hat{g})]^{-\mu_1 \gamma} Z_0[w \mathcal{L}(\hat{t}, \hat{g})], \quad (5.23)$$

where C_G is the critical amplitude at $\hat{g}=0$, the leading exponent is given by

$$\gamma = -\lambda_0/\lambda_1, \quad (5.24)$$

while the logarithmic dependence is contained in

$$\mathcal{L}(\hat{t}, \hat{g}) = 1/[1 + (D/\lambda_1) w \ln(\hat{t}/w^{\mu_1})], \quad (5.25)$$

where, to recapitulate, $w = \hat{t}^{k_1} \hat{g}^{k_2}$. [Compare with (5.11) and (5.20).] The scaling function $Z_0(w)$ [which derives from $X(w)$ in Appendix C] is normalized so that $Z_0(0) = 1$: it should have an expansion for small w that ensures that $G(t, g)$ has a simple power series in g (at $g = 0$) when $t > 0$; see further below.

Before discussing the significance of this result for the Ising model, it is useful to note some of the limitations of the model equations we have solved and indicate the modifications that can result in a more general situation. We comment briefly on three aspects: (i) Only two fields, one relevant and one irrelevant, have been considered in our model. A more complete description would include, for example, the effects of the ordering field h , whose presence in the full temperature-like nonlinear scaling field can be shown¹⁷ to lead to additive terms proportional to $|t|^{1-\alpha}$ in the ordering susceptibility; these behave as $t \ln|t|$ in the $d = 2$ Ising model. (ii) Despite the appearance of terms like $\ln \hat{t}$ and $\ln \hat{g}$ in thermodynamic quantities, the model equations yield no logarithms in the equation for the critical locus, $t_c(g)$, itself: this is given by $\hat{t}(t, g) = 0$, and since \hat{t} is a C_∞ function of \bar{t} and \bar{g} , no logarithms appear. In fact, one can see that this is always the case for any pair of flow equations with one relevant and one irrelevant field. If, however, two (or more) irrelevant fields enter, logarithms can also appear in the equation for the critical surface.⁴⁰ (iii) In writing (5.21) we have not considered the most general renormalization equation for G . For instance, terms representing additive renormalization can lead to additive logarithms in the result.⁴⁰ (This is the mechanism yielding the logarithmic specific heat of the pure Ising model.¹)

C. Ising-like scaling and the pure Ising model

Let us, finally, consider the logarithmic renormalization-group scaling form (5.23) as a candidate for describing the susceptibility $\chi(T, g)$ [identified as $G(T, g)$] of the KI and DG Ising-like models in the vicinity of the pure Ising limit, $g = 0$. As discussed, we must now identify $\hat{t}(t, g)$ as an *intermediate* nonlinear scaling field which is a polynomial in t and g reducing to the linear scaling field \bar{t} defined in (5.1) for small t and g . Likewise, $\hat{g}(t, g)$ must be a polynomial reducing to g and, in light of (5.8), satisfying

$$\hat{g}(t, g) = g[1 + O(g, t)], \quad (5.26)$$

so that $g = 0$ (or $y = 1$) is the full nonlinear scaling axis.

If one accepts $\theta = \frac{4}{3}$ and acknowledges $\lambda_1 \equiv 1/\nu = 1$ as the thermal (or energy) renormalization-group eigenvalue, one has $\lambda_2 = \frac{4}{3}$ and the appropriate choice for (k_1, k_2) is (4, 3). Then t and g appear only in the scaling combination $w = \hat{g}^3 \hat{t}^4$, except in the argument of the logarithm in (5.25), where one finds $\hat{g}^3 \hat{t}^\psi$ with $\psi = 4 - 1/\mu_1$.

It is worth commenting that quite equivalent results would obtain if we supposed that g itself did not couple directly to a critical operator but that $g^{k_2} \equiv g^3 = u_3$ was the field which coupled to a critical operator, which, in that case, would have an eigenvalue $\lambda_3 = k_2 \lambda_2 = -4$. This is more palatable as regards the known behavior of the

pure Ising model since such irrelevant operators do in fact arise (for example via lattice differences).^{42, 19} The resonance condition would then be $4\lambda_1 + \lambda_3 = 0$, but one would still have $w = \hat{u} \hat{t}^4 = \hat{g}^3 \hat{t}^4$.

Now, provided only integral powers of w appear in the expansion of the scaling function $Z_0(w)$ in (5.23), it is clear that the desired absence of the unseen factors $t^{1/3}$ and $t^{2/3}$ at $g = 0$ is ensured not only in $\chi(T, 0)$ itself, but also in all the derivatives $(\partial^k \chi / \partial g^k)_{g=0}$. On the other hand, the presence of logarithmic terms of the form $\hat{g}^3 \hat{t}^4 \ln \hat{t}$ in (5.25) means that additive logarithmic terms of the form $g^{3k} \hat{t}^{4k - \gamma} (\ln \hat{t})^{k-j}$ should appear in $\chi(T, g)$ for all $k = 1, 2, 3, \dots$ and $j = 0, 1, \dots, k - 1$ whenever $g \neq 0$. These "correction-to-scaling" terms vanish, however, at $g = 0$, which clearly identifies $g = 0$ as a multisingular point. On the other hand, one should, for example, be able to find a term varying as $t^{4-\gamma} \ln t$ in $(\partial^3 \chi / \partial g^3)_{g=0}$ and as $t^{8-\gamma} (\ln t)^2$ in $(\partial^6 \chi / \partial g^6)_{g=0}$. These expectations could be checked by explicit calculations for the pure Ising model. The appearance of such logarithms appears very reasonable in view of the fact that they are already known to appear in the individual Ising spin-correlation functions. More explicitly, the spin-spin-correlation function $\langle s(\mathbf{0})s(\mathbf{R}) \rangle$ in the pure Ising model can be expressed in terms of Toeplitz determinants of an order that (on average) increases linearly with the separation $|\mathbf{R}|$.¹³ Each individual Toeplitz matrix element behaves like the mean thermodynamic energy exhibiting the (precise) critical behavior

$$A_{ij} + t B_{ij}(t) \ln |t| + t C_{ij}(t),$$

where B_{ij} and C_{ij} are analytic functions of t . Clearly, then, $\langle s(\mathbf{0})s(\mathbf{R}) \rangle$ contains $t^k (\ln t)^{k-j}$ singularities with $k \sim |\mathbf{R}|$. Similar remarks apply to the higher-order correlation functions needed to evaluate $(\partial^k \chi / \partial g^k)_{g=0}$.

Lastly, a further remark about the nature of the scaling function $Z_0(w)$ is in order. The point is that for $\hat{t} > 0$ the right-hand side of (5.23) must produce no terms involving factors of $\ln g$ as $g \rightarrow 0$ with $t > 0$ since these would imply nonanalytic behavior in g above $T_c(g)$, which is not physical. This means that the scaling function itself must contain logarithmic terms so as to cancel the $\ln \hat{g}$ terms arising from the \mathcal{L} functions in (5.23). Specifically, one can check that if

$$\begin{aligned} Z_0(w) = & 1 + Z_{1,1} w \ln w + Z_1 w + Z_{2,2} w^2 (\ln w)^2 \\ & + Z_{2,1} w^2 \ln w + Z_2 w^2 + O(w^3 \ln^3 w), \end{aligned} \quad (5.27)$$

then the leading $\ln g$ and $(\ln g)^2$ terms cancel, provided

$$Z_{1,1} = D\mu_1^2 \gamma / \lambda_1 \quad \text{and} \quad Z_{2,2} = -\frac{1}{2} D^2 \mu_1^3 \gamma (1 + \mu_1 \gamma) / \lambda_1^2, \quad (5.28)$$

while appropriate values of $Z_{2,1}$, etc., serve to cancel higher-order logarithmic terms.

In summary, the numerical and analytical evidence is consistent with the corrections to scaling in the two-dimensional Klauder and double-Gaussian models being purely logarithmic in character for $g \neq 0$ ($y \neq 1$), but with amplitudes that vanish on approach to the pure Ising lim-

it ($g=0$) in a way described by an apparent correction-to-scaling exponent $\theta = \frac{4}{3}$.

VI. BORDER MODELS AND INCIPIENT MULTICRITICALITY

In Sec. III we reported the observation of an effective exponent $\gamma_{\text{eff}} \simeq 1.95$ in *single*-variable analysis of the K1, DG, and $\lambda\varphi^4$ models for intermediate values of y and λ (see Fig. 1). In their single-variable analysis (using shorter series than available to us¹⁶) of the $\lambda\varphi^4$ model at a theoretically identified^{27(b)} “border” value, $\lambda = \lambda_b$, that corresponds to $u_2 \equiv 0$ in (2.31), Baker and Johnson^{27(a)} found similar values of γ_{eff} . They cited their observations as evidence that “critical exponent universality fails for the two-dimensional continuous spin Ising model. . . contrary to what has previously been assumed.” Specifically, they claim that the $\lambda_b\varphi^4$ border model is in a different universality class than the standard Ising model having $\gamma_b \simeq 2.00$ in place of $\gamma_I = 1.750$: they quote the range 1.89 to 2.02 for γ_b and suggest, in our notation, $\theta_b \simeq 0.90$ to 0.99. We believe that such a conclusion is premature at best: Indeed, the balance of the evidence, which we review below, seems to support the alternative interpretation which reads the observation of $\gamma_{\text{eff}} \simeq 1.95$ as merely symptomatic of strong Gaussian-to-Ising crossover effects. The true asymptotic exponent would then be $\gamma = \gamma_I$ for all nonzero values of y or λ , in accord with the standard picture. Nevertheless, for strong enough deviations of the single-spin weighting function, $W_X(s)$, from the K1, DG, or $\lambda\varphi^4$ forms, other types of critical behavior must arise so that the full span of behavior encompassed by $O(1)$ continuous-spin Hamiltonians with nearest-neighbor couplings does, surely, include more than just Ising and Gaussian criticality. Accordingly, we also make some comments about the possible role of scalar tricriticality in the observed crossover behavior.²⁶ (Related considerations by Baker^{27(c)} should also be mentioned.)

Recall, first, the fact that the two-variable PDA methods are intrinsically better able to address questions of crossover *versus* new types of criticality than are single-variable methods. Further, our PDA study provides definite evidence favoring asymptotic Ising-like critical behavior for all $0 < y \leq 1$ for the Klauder and double-Gaussian models. Thus, as discussed in Sec. III, the majority of approximants computed exhibit flow patterns isomorphic to those in Figs. 2 and 3, with a critical trajectory that flows directly from the Gaussian multicritical point, G , to an Ising-like multicritical point, C , thus implying that the entire critical locus from G up to and through C is Ising-like. On the other hand, a minority of the approximants do display an extra fixed point, B , on the critical trajectories linking G and C , which might well be viewed as supportive of the Baker-Johnson contention. However, as explained in Sec. III, the associated flow patterns are most often defective, inasmuch as another, unphysical locus of singularities, DB [in Figs. 4(a) and 4(b)], is also present: This suggests that the appearance of B itself should be regarded as a defect, a viewpoint which is supported by the wide numerical range of associated crossover exponents $\phi_B \equiv -\theta_B$ which is found. Further-

more, the critical behavior implied by this class of approximants is Ising-like on the critical line between B and C , but Gaussian-like between B and G . This latter, “asymptotically free” behavior is difficult to reconcile with the results of perturbation theory around the Gaussian limit. As discussed in Sec. II, the exact perturbative results for $(\partial\chi/\partial y)_{y=0}$, etc., are fully consistent with the standard field-theoretic picture of an *unstable* Gaussian fixed point with a positive crossover exponent $\phi_G = \frac{1}{2}\epsilon \equiv \frac{1}{2}(4-d)$. An unstable fixed point indicates crossover to a new type of critical behavior, inconsistent with the Gaussian-like, asymptotic freedom implied by those approximants exhibiting a border multisingularity, B . In principle, however, one might have a Gaussian-to-Gaussian crossover *at or, perhaps, very close to* $y=0$; thus the argument is not totally convincing. However, it would still seem very difficult to explain such behavior in what is, after all, a weak-coupling regime where the field-theoretic picture may even be susceptible of rigorous proof.

Another argument casting doubt on the existence of a new, non-Ising universality class, at least within the double-Gaussian model, invokes the exact factorizability³¹ of the DG partition function. As discussed in Sec. II, the critical properties of the DG model are identical to those of a “range” model that is a standard ($s_i = \pm 1$) Ising model with ferromagnetic pairwise interactions that decay exponentially with distance. Such interactions can support only the orthodox type of Ising order. One knows, e.g., by comparing the exact results for honeycomb, square, and triangular Ising lattices,¹³ that adding ferromagnetic short-range interactions normally has no effect on the nature of the criticality. Renormalization-group arguments, supported by exact spherical model, results for all d , etc., suggest strongly that exponentially decaying interactions should be equivalent to strictly short-range interactions. In summary, it seems most likely that the range model, and hence the DG model for $y > 0$, is in the same universality class as the pure Ising model with only nearest-neighbor couplings.

Finally, the close numerical similarity of the $\lambda\varphi^4$, DG, and K1 spin weight functions as they each interpolate smoothly between the single-peaked Gaussian weight and the infinitely sharp double peaks of the pure Ising limit, leads us to believe that the conclusions for the latter two models should apply equally to the former. For the reasons given we thus feel it is more fitting to ascribe the observations of $\gamma_{\text{eff}} \simeq 1.95$ for intermediate y and λ in the $\lambda\varphi^4$, DG, and K1 models to crossover effects rather than to invoke a new universality class.

Let us round out the discussion, however, by looking a little further into one other type of (multi-) critical behavior that should arise in two-dimensional scalar spin systems even if it does not occur in that part of Hamiltonian space spanned directly by the K1, DG, and $\lambda\varphi^4$ models. (A schematic representation of the space of Hamiltonians illustrating the relation between various models, including the general spin Ising model,^{8,43} is given in Fig. 2 of Ref. 26.) Specifically, we wish to discuss a natural extension of the DG model, which should encompass *tricriticality*. To this end we first define modified

single-spin weight functions by writing the full partition function as

$$Z_X = \int \prod_i ds_i \tilde{W}_X(s_i) \exp \left[\frac{1}{2} \sum_{(i,j)} K_{ij} (s_i - s_j)^2 \right]. \quad (6.1)$$

By matching this to (2.1), one finds

$$\tilde{W}_X(s) \equiv \exp \left[\frac{1}{2} \hat{K}(0) s^2 \right] W_X(s), \quad (6.2)$$

where $\hat{K}(\mathbf{q})$ is defined as in (2.11). The point of rewriting Z in this way is that the net single-site energy, $\ln[\tilde{W}_X(s)]$, is thereby exhibited explicitly. For appropriate *block* spin variables S_j , the existence of a universal net weight function $\tilde{W}(S)$ governing the fixed-point distribution of spins is fairly well established.⁴⁴ Furthermore, there are indications that some properties of even the net *single*-spin distribution, $\tilde{W}_X(s)$, are quasiuniversal, provided one confines attention to Hamiltonians with only nearest-neighbor interactions. To explore this feature, it is reasonable to characterize a weight function by its reduced moments

$$\tilde{M}_n^X = \int \tilde{W}_X(s) s^n ds / \left[\int \tilde{W}_X(s) s^2 ds \right]^{n/2}, \quad (6.3)$$

normalized so that $\tilde{M}_2^X \equiv 1$.

An example of the quasiuniversality exhibited by single-spin distribution functions is provided by the K1 and DG models at their Ising-like multicritical point. In two dimensions, the identity of $\tilde{W}_{K1}(s)$ and $\tilde{W}_{DG}(s)$ is immediate if, as we have argued, the multicritical point for both models coincides with the pure Ising critical point. In three dimensions (where the quasiuniversality was first noticed⁴⁵) PDA study¹⁰ yields the Ising-like multicritical values $x_c(K1) \simeq x_c(DG) \simeq 1.21$ and $y_c(K1) \simeq 0.81$, $y_c(DG) \simeq 0.90$. From these, one finds

$$\tilde{M}_4 \simeq 1.37 \text{ (K1)}, \quad 1.34 \text{ (DG)}, \quad (6.4)$$

$$\tilde{M}_6 \simeq 2.43 \text{ (K1)}, \quad 7.00 \text{ (DG)}. \quad (6.5)$$

The originally unanticipated near equality of the fourth moments here indicates the quasiuniversality. The sixth moments, however, necessarily differ by virtue of the fact that we have restricted the Hamiltonians to the submanifolds spanned by the K1 and DG models.

Now consider the Blume-Capel model:⁴⁶ this is a spin-1 Ising model ($s_i = 1, 0, -1$) with nearest-neighbor coupling $Ks_i s_j$ and a single-spin term Δs_i^2 . It can be described by the weight function

$$\begin{aligned} \tilde{W}_{BC}(s) = & 2(w-1)\delta(s) \\ & + [\delta(s + \sqrt{w}) + \delta(s - \sqrt{w})] \exp \left[\frac{1}{2} \hat{K}(0) s^2 \right], \end{aligned} \quad (6.6)$$

in which the parameter w stands in for the single-spin (or crystal-field) parameter.⁴⁷ This model certainly has a *tricritical* point; a recent study⁴⁸ reports the tricritical values $x_t(BC) \simeq 0.573$ and $w_t(BC) \simeq 10.61$, which yield the moments

$$\tilde{M}_4 \simeq 1.46 \text{ and } \tilde{M}_6 \simeq 2.13 \text{ (BC, tricrit.)}. \quad (6.7)$$

We take these values as an indication of the location of the tricritical manifold in the space of Hamiltonians: note

that these moments differ significantly from (6.4) and (6.5).

We now raise the question:²⁶ "Might the strong crossover effects observed in the 'border regions' of the K1, DG and $\lambda\varphi^4$ models, where γ_{eff} attains a maximum, be associated with incipient tricriticality?" To shed some light on this question, we may evaluate the moments corresponding to the border values $x_b \simeq 1.20$ (K1), 1.19 (DG), 1.32 ($\lambda\varphi^4$, Ref. 27) and $y_b \simeq 0.30$ (K1), 0.50 (DG), and $\lambda_b \simeq 0.1142$ ($\lambda\varphi^4$, Ref. 27). We find

$$\tilde{M}_4 \simeq 2.40 \text{ (K1)}, \quad 1.99 \text{ (DG)}, \quad 1.58 \text{ } (\lambda\varphi^4), \quad (6.8)$$

$$\tilde{M}_6 \simeq 9.12 \text{ (K1)}, \quad 5.57 \text{ (DG)}, \quad 3.02 \text{ } (\lambda\varphi^4). \quad (6.9)$$

These values vary quite strongly, but in a regular way, which suggests a monotonic approach to the tricritical region located by (6.7). (See also Fig. 2 of Ref. 26.)

This observation suggests that it might be the relatively close approach of the K1, DG, and $\lambda\varphi^4$ border models to a tricritical manifold that plays a role in determining the behavior of γ_{eff} (as exhibited in Fig. 1). This proposed association would also rationalize the appearance of PDA flow patterns of type *B*, containing the extra fixed point *B*; the fraction of such approximants found increases in going from the K1 to the DG model. This might reflect the closer proximity to the tricritical manifold and the associated stronger crossover effects in the latter case. Perhaps *B* itself could be interpreted as an approximate, but premature representation of an incipient tricritical point.

To investigate these speculations it is desirable to generalize the K1, DG, and $\lambda\varphi^4$ models so as to encompass genuine tricriticality. Many such generalizations are possible, but a particularly appealing one is obtained by applying the procedure of Gaussian smearing³³ to the Blume-Capel weight function (6.6): This yields

$$\begin{aligned} W_3(s; y, w) = & 2(w-1) \exp(-s^2/2g) + \exp[(s + \sqrt{wy})^2/2g] \\ & + \exp[(s - \sqrt{wy})^2/2g], \end{aligned} \quad (6.10)$$

where, again, $g = 1 - y$. Consider this weight function combined with a nearest-neighbor coupling: The model reduces to the Gaussian model when $y = 0$, to the Blume-Capel model when $y = 1$, and to the double-Gaussian model when $w = 1$. Now, the tricritical point in the Blume-Capel model is presumably drawn out into a tricritical locus in the full three-parameter (w, x, y) space. It would be important to know the location and orientation of this tricritical locus relative to the double-Gaussian plane ($w = 1$) if the associated crossover effects are to be understood quantitatively. Thus, the observed values of γ_{eff} close to 2.0 might possibly result from an approximate tangency of a locus at fixed y in or near the double-Gaussian plane, to the tricritical locus; a precise tangency of this sort would imply a doubled value, $\gamma \simeq 2.06$, of the standard tricritical susceptibility exponent⁴⁹ $\gamma_t = \frac{37}{36} \simeq 1.03$. To support (or destroy) such a speculation, however, a study of the full (w, x, y) space seems imperative. Even if successful, it might well still leave one with the conclusion that only normal crossover effects are visible in the simple Ising-like models considered here. Con-

versely, some more exotic form of multicriticality might come clearly to view: we feel, however, that the simpler possibilities should be explored first.

VII. CONCLUSIONS

Our study of the $O(1)$ Klauder and double-Gaussian models in two dimensions has addressed two distinct issues; our primary concern has been the nature of the corrections to leading power-law behavior in the vicinity of the pure spin- $\frac{1}{2}$ Ising limit: Secondly, we have considered the strong crossover effects apparent in these models in the intermediate parameter range between the Gaussian and Ising extremes. Analysis of a wide range of partial-differential approximants has led to the notion that for $d=2$ (in contrast to $d=3$) the pure spin- $\frac{1}{2}$ Ising model plays a special role: Explicitly, the Onsager critical point appears as a *multicritical* point in the full parameter space, and the Ising axis ($y=1$) is an axis for the nonlinear scaling fields describing Ising-like criticality. Moreover, the numerical results support Nienhuis's conjecture that the leading corrections are described by an exponent $\theta=\frac{4}{3}$. To reconcile the absence of terms like $(T-T_c)^{1/3}$ and $(T-T_c)^{2/3}$ in exact calculations for the pure Ising model with this result, we propose that a resonance between two renormalization-group eigenvalues leads to *logarithmic* singularities in the nonlinear scaling fields (in contrast to simple power-series expansions). Such an effect should occur whenever θ is a rational fraction and, in turn, yields logarithmic correction factors in the critical behavior of thermodynamic functions away from the pure Ising limit. The proposed logarithmic structure may be probed by computing sums of appropriate correlation functions of the pure Ising model, and may thus be checked by explicit calculations which, clearly, would be valuable to have.

Our single-variable analysis of the Klauder, double-Gaussian, and $\lambda\varphi^4$ models yields a maximal value for the effective susceptibility exponent of $\gamma_{\text{eff}}\simeq 1.95$, for intermediate values of the parameter y . However, the two-variable PDA analysis provides evidence that there is only a single (Ising-like) universality class away from the Gaussian limit of the KI and DG models and, by numerical similarity, for the $\lambda\varphi^4$ models also. In a speculative vein it was suggested that the strong crossover effects might be associated with incipient tricriticality in these models: Calculation of moments of the critical-point single-spin weight functions provides some evidence for this, but a systematic consideration of this idea would involve enlarging the parameter space so as to ensure the presence of genuine tricriticality. A suitably extended model was defined which would be interesting to study in the hope of elucidating how close the "border" models lie to a tricritical or other type of manifold.

ACKNOWLEDGMENTS

We are most grateful to B. G. Nickel for providing us with the extensive two-variable series studied; without these our numerical work would have been impossible. We have benefited from helpful discussions and

correspondence with J.-H. Chen, D. A. Huse, B. G. Nickel, V. Privman, M. Randeria, S. Shenker, and D. F. Styer. The support of the National Science Foundation, principally through the Applied Mathematics program, is gratefully acknowledged.

APPENDIX A: NEAR THE ISING LIMIT

In this appendix we establish the relation (2.16) between the single-spin partition functions of the double-Gaussian and Klauder models, to first order in the deviations g from the Ising limit $y=1$.

It is easy to calculate $Z_{\text{DG}}^0(h;y)$ [see (2.6)] since each of the two separate integrals resulting from (2.3) is Gaussian in form: One obtains

$$Z_{\text{DG}}^0(h;y) = \cosh(h\sqrt{y})e^{gh^2/2}, \quad (\text{A1})$$

where we have normalized by dividing by $Z_{\text{DG}}^0(0;y)$. On expanding this to first order in g , one recovers the first part of (2.16).

It is not quite as straightforward to evaluate

$$Z_{\text{KI}}^0(h;y) \propto \int_{-\infty}^{\infty} ds e^{hs} |s|^{y/g} e^{-s^2/2g}. \quad (\text{A2})$$

However, it may be rewritten as

$$Z_{\text{KI}}^0(h;y) \propto \int_0^{\infty} \frac{dt}{t} \cosh(ht) e^{\phi(t)/g}, \quad (\text{A3})$$

with

$$\phi(t) = \ln t - \frac{1}{2}t^2 = -\frac{1}{2} - (t-1)^2 + O((t-1)^3). \quad (\text{A4})$$

When $g \rightarrow 0$ the integrand becomes sharply peaked about $t=1$ and, setting $t-1=u\sqrt{g}$, the integral can thence be evaluated by the method of steepest descents. Carrying this through to first order in g yields the second part of (2.16).

APPENDIX B: FLOW PATTERNS WITH EXTRA FIXED POINTS

In Sec. III we pointed out that a significant minority of PDAs exhibit additional fixed points B (on the critical locus) and D (on the Gaussian axis) in addition to the Gaussian and Ising fixed points G and C (see Fig. 4). In this appendix we discuss some implications of such flow patterns, and, in particular, the nature of the singularity on the segment of trajectory DB .

Before taking up the patterns in Figs. 4(a) and 4(b) separately, let us remark on a feature common to both, namely that the exponent γ_D which characterizes the singularity of the susceptibility along the $y=0$ axis near D is identically zero. This follows because the Gaussian model susceptibility, $\chi_G=1/(1-x)$, is nonsingular for $x < 1$, and the exact Gaussian form was imposed on the PDAs under discussion. Explicitly, we must have $Q(x_D,0)=0$ at the fixed point D , but in view of the Gaussian axis constraints (3.8) and (3.9), and (3.15) and (3.16), it follows that

$$Q(x_D,0) = x_D(1-x_D)P(x_D,0). \quad (\text{B1})$$

Hence, for $0 < x_D < 1$, we must have $P(x_D, 0) = 0$ and thus (using results from Ref. 12, etc.) $\gamma_D = -P(x_D, 0)/\lambda_1$ also vanishes.

Now let us turn to the individual flow patterns. In Fig. 4(a) the fixed point B is bicritical¹² in character and thus exhibits a "radial" flow pattern. Around B , the scaling form

$$\chi \approx C \tilde{t}^{-\gamma_B} Z_B(z) \quad (\text{B2})$$

holds,^{1,10} with

$$z = \tilde{g}/\tilde{t}^{\phi_B}, \quad (\text{B3})$$

where \tilde{g} and \tilde{t} are nonlinear scaling fields asymptotically equal to the linear scaling fields \bar{g} and \bar{t} defined with an origin at B and axes labeled as shown in the figure. The susceptibility must be nonanalytic along the loci BC and BD since the approach to these loci is governed by the flows into fixed points C and D , respectively. Now C is a fixed point of Ising character implying that the critical behavior all along BC is also Ising-like. At fixed point D , on the other hand, γ_D vanishes and the leading singular behavior is that characterized only by the corrections to scaling. Hence, if t_D measures the deviation from the locus DB , we will have

$$\chi = C_D (1 + a_D t_D^{\theta_D} + \dots). \quad (\text{B4})$$

The two different types of critical behavior (along DC and DB) manifest themselves¹² as two different singularities of the scaling function,¹² Z_B , at finite values of z , say z^+ and z^- .

Although the singularity across the locus BD seems highly unphysical, as discussed in the text, it is comparatively weak (typical values of θ_D ranging from 0.01 to 0.30). Furthermore, since, as argued in the text, D most probably represents a *defect*, it should not, as such, be allowed to introduce spurious singularities into the integrated approximant as occurs in (B4). This can, indeed, be accomplished within the spirit of PDA analysis by matching the flows from B on a locus which runs above D up to some value $x > x_D$: Then the singular amplitude a_D in (B4), and all higher singularities, would vanish *identically*. Thus it is appropriate to consider the continuation of $\chi(x, y)$ beyond the locus BD into the region BDG . Similar arguments then show that the locus BG must be singular and, indeed, exhibit a divergent Gaussian-like singularity with $\gamma_G = 1$. This singularity *cannot* reasonably be removed by choice of boundary-matching locus.

Consider now the situation illustrated in Fig. 4(b). Flows around the fixed point B are hyperbolic: The scaling form (B2) is still valid, but the crossover exponent ϕ_B is now *negative*, so that it is appropriate to define

$$\theta_B = -\phi_B > 0. \quad (\text{B5})$$

Furthermore, the \bar{t} and \bar{g} axes coincide asymptotically with the loci BD and BC , respectively. As in the case shown in Fig. 4(a), the susceptibility must be singular along BC , with Ising-like critical behavior. This has the important consequence that the scaling function $Z_B(z)$ must be singular at $z = 0$: In fact, recalling the fact that

$z = \tilde{g} \tilde{t}^{-\theta_B}$, one finds that one must have

$$Z_B(z) \approx Z^0 z^{(\gamma_B - \gamma_I)/\theta_B} \quad \text{as } z \rightarrow 0 \quad (\text{B6})$$

in order to reproduce the singular behavior $\chi \sim t^{-\gamma_I}$, where t represents the deviation from the critical locus BC with $t \approx \tilde{t}$ near B . From (B6) and (B2) it follows that χ is also singular along the locus DB , and so at a fixed or slowly varying value of \tilde{t} one has

$$\chi \sim \tilde{g}^\psi \sim t_D^\psi \quad \text{with } \psi = (\gamma_B - \gamma_I)/\theta_B. \quad (\text{B7})$$

Depending on the relative magnitudes of γ_B and γ_I , the susceptibility χ may thus diverge ($\gamma_B < \gamma_I$) or attain a finite value in a singular fashion ($\gamma_B > \gamma_I$) as the locus BD is approached, i.e., when $t_D \rightarrow 0$.

APPENDIX C: INTEGRATION OF THE MODEL FLOW EQUATIONS

In this appendix we present some details of the solution of the model flow equations (5.14) and (5.15) which illustrate the phenomenon of resonance for rational θ . For notational convenience, we denote \hat{t} and \hat{g} by t and g here. The first step is to define

$$t' \equiv t e^{-\lambda_1 l}, \quad g' \equiv g e^{-\lambda_2 l}, \quad (\text{C1})$$

which then satisfy

$$\frac{1}{D_1} \frac{d}{dl} (\ln t') = \frac{1}{D_2} \frac{d}{dl} (\ln g') = t'^{k_1} g'^{k_2}. \quad (\text{C2})$$

On setting

$$w(l) = t'^{k_1} g'^{k_2} \equiv t^{k_1} g^{k_2}, \quad (\text{C3})$$

we find that (C2) implies

$$w(l) = w_0 / (1 - D w_0 l) \quad (\text{C4})$$

and

$$[g'(l)/g_0]^{D_1} = [t'(l)/t_0]^{D_2}, \quad (\text{C5})$$

where D is defined in (5.18) and the subscript 0 denotes, here and below, evaluation at $l = 0$. From these results the solutions (5.16) and (5.17) follow immediately.

To understand the resulting thermodynamics we follow standard procedures and renormalize up to a *matching value*, $l^\dagger(t_0, g_0)$, defined as the solution of the equation

$$G[t(l^\dagger), g(l^\dagger)] = G^\dagger, \quad (\text{C6})$$

where G^\dagger is fixed noncritical, reference value of a selected thermodynamic (or other) variable, which, following the text, we may suppose obeys the multiplicative flow equation (5.21). To solve this equation for l^\dagger , consider first the simple case $D = 0$ and set

$$V_1(t_0, g_0) = e^{l^\dagger t_0^{1/\lambda_1}}. \quad (\text{C7})$$

Using the solutions (5.16) and (5.17) then yields

$$G(V_1^{\lambda_1}, V_1^{\lambda_2} w_0^{1/k_2}) = G^\dagger, \quad (\text{C8})$$

from which it is clear that V_1 is actually a function only of w_0 . By solving (C8) for l^\dagger and normalizing by defining t^\dagger as the root of

$$G(t^\dagger, 0) = G^\dagger, \quad (\text{C9})$$

we obtain, for $D = 0$,

$$l^\dagger(t_0, g_0) = (1/\lambda_1) \ln(t^\dagger/t_0) + \ln V_0(w_0), \quad (\text{C10})$$

where $V_0(0) = 1$ and $V_0(z)$ should have a formal expansion in powers of w_0^{1/k_2} since $G(t, g)$ should be analytic in g for $\tilde{t} > 0$.

To obtain a solution for $D \neq 0$ we generalize (C7) in the light of (5.16) by defining

$$V(t_0, g_0) = e^{t^\dagger t_0^{1/\lambda_1}} / (1 - Dw_0 l^\dagger)^{\mu_1/\lambda_1}, \quad (\text{C11})$$

and then, from (5.17), we obtain

$$g(l^\dagger) = V^{\lambda_2} [w_0 / (1 - Dw_0 l^\dagger)]^{1/k_2}, \quad (\text{C12})$$

where we have used $k_1 \mu_1 + k_2 \mu_2 = 1$, which follows from (5.19). Substituting, as before, in (C6) we now find that V is a function only of the combination $v = (1 - Dw_0 l^\dagger)/w_0$

appearing in (C12). Then one can rearrange (C11) and solve formally to obtain

$$v/D \equiv 1/Dw_0 - l^\dagger = W[w_0 \mathcal{L}(t_0, g_0); D], \quad (\text{C13})$$

where $\mathcal{L}(t_0, g_0)$ is the logarithmic function defined in (5.25) which approaches unity when $D \rightarrow 0$. The function $W(u; D)$ represents a reincarnation of the scaling function. To cast this result in a more useful form we note that it must reduce to (C10) when $D \rightarrow 0$. For this to occur, W has to take the form

$$W(u; D) = 1/Du - (1/\lambda_1) \ln(u^{\mu_1}/t^\dagger) + \ln X(u; D), \quad (\text{C14})$$

where $X(0; 0) = 1$ and $X(w; D)$ should have a power-series expansion in w^{1/k_2} up to order k_2 . On using this and solving (C13) for l^\dagger , we finally obtain

$$e^{t^\dagger} = (t^\dagger/t_0)^{1/\lambda_1} [\mathcal{L}(t_0, g_0)]^{-\mu_1/\lambda_1} X[w_0 \mathcal{L}(t_0, g_0)], \quad (\text{C15})$$

in which, to recapitulate, $w_0 = t_0^{k_1} g_0^{k_2}$, and we have omitted the explicit D dependence of X .

*Permanent address: Tata Institute of Fundamental Research, Homi Bhabha Road, Bombay 400005, India.

¹F. J. Wegner, Phys. Rev. B 5, 4529 (1972).

²K. G. Wilson and M. E. Fisher, Phys. Rev. Lett. 28, 240 (1972).

³A. A. Vladimirov, D. I. Kazakov, and O. V. Tarasov, Zh. Eksp. Teor. Fiz. 77, 1035 (1979) [Sov. Phys.—JETP 50, 521 (1979)].

⁴(a) J. C. Le Guillou and J. Zinn-Justin, Phys. Rev. B 21, 3976 (1980); (b) J. Zinn-Justin, in *Phase Transitions: Cargèse 1980*, edited by M. Lévy, J. C. Le Guillou, and J. Zinn-Justin (Plenum, New York, 1982), p. 169.

⁵S. G. Gorishny, S. A. Larin, and F. V. Tkachov, Phys. Lett. 101A, 120 (1984).

⁶(a) G. A. Baker, Jr., B. G. Nickel, M. S. Green, and D. I. Meiron, Phys. Rev. Lett. 36, 1351 (1976); (b) G. A. Baker, Jr., B. G. Nickel, and D. I. Meiron, Phys. Rev. B 17, 1365 (1978).

⁷(a) B. G. Nickel, in *Phase Transitions: Cargèse 1980*, Ref. 4(b), p. 291; (b) B. G. Nickel, Physica 106A, 48 (1981).

⁸J. Zinn-Justin, J. Phys. (Paris) 40, 63 (1979).

⁹The advent of Nickel's 21st-order series was crucial in resolving the disagreement between field-theoretic predictions and earlier estimates based on long, but not such long, series; see, e.g., D. S. Gaunt and M. F. Sykes, J. Phys. A 12, L25 (1979). A number of subsequent biased analyses of the longer series yielded results compatible with Ref. 7; see, e.g., R. J. Roskies, Phys. Rev. B 24, 5305 (1981); J. Adler, M. Moshe, and V. Privman, *ibid.* 26, 3958 (1982).

¹⁰J.-H. Chen, M. E. Fisher, and B. G. Nickel, Phys. Rev. Lett. 48, 630 (1982).

¹¹(a) M. E. Fisher, Physica 86-88, 590 (1977); (b) M. E. Fisher and R. M. Kerr, Phys. Rev. Lett. 39, 667 (1977).

¹²M. E. Fisher and J.-H. Chen, in *Phase Transitions: Cargèse 1980*, Ref. 4(b), p. 169.

¹³B. M. McCoy and T. T. Wu, *The Two-Dimensional Ising*

Model (Harvard University Press, Cambridge, Mass., 1973).

¹⁴L. Onsager, Phys. Rev. 65, 17 (1944).

¹⁵E. Barouch, B. M. McCoy, and T. T. Wu, Phys. Rev. Lett. 31, 1409 (1973).

¹⁶B. G. Nickel (private communication); see also B. G. Nickel and J. J. Rehr (unpublished).

¹⁷A. Aharony and M. E. Fisher, Phys. Rev. Lett. 45, 679 (1980); Phys. Rev. B 7, 4394 (1983).

¹⁸B. Nienhuis, J. Phys. A 15, 199 (1982).

¹⁹D. Friedan, Z. Qiu, and S. Shenker, Phys. Rev. Lett. 52, 1575 (1984).

²⁰G. E. Andrews, R. J. Baxter, and P. J. Forrester, J. Stat. Phys. 35, 193 (1984).

²¹D. A. Huse, Phys. Rev. B 30, 3908 (1984), and private communication.

²²There is an error in Eq. (4.16) of Ref. 6(b): the value appearing there should be doubled.

²³J. Adler and I. G. Enting, J. Phys. A 17, 2233 (1984).

²⁴V. Privman (private communication).

²⁵J. M. Debierre and L. Turban, Phys. Lett. 97A, 235 (1983).

²⁶A brief account of our work has appeared [M. Barma and M. E. Fisher, Phys. Rev. Lett. 53, 1935 (1984)].

²⁷(a) G. A. Baker, Jr. and J. D. Johnson, J. Phys. A 17, L275 (1984); see also (b) G. A. Baker, Jr., J. Math. Phys. 24, 143 (1983) and (c) J. Phys. A 17, L621 (1984).

²⁸M. E. Fisher, Physica 25, 521 (1959).

²⁹J. R. Klauder, Ann. Phys. (N.Y.) 117, 19 (1979); see Eq. (3.27); in our use of the model we set the quartic, φ^4 , term to zero.

³⁰There is a misprint in the definition of $b^2(y)$, after Eq. (5) in Ref. 10; Eq. (2.5) of the present text is correct.

³¹G. A. Baker, Jr. and A. R. Bishop, J. Phys. A 15, L201 (1982).

³²B. G. Nickel (private communication).

³³M. Barma, J. Phys. A 16, L745 (1983).

³⁴We are indebted to Dr. J.-H. Chen for pointing this out.

- ³⁵See, e.g., G. A. Baker, Jr., in *The Padé Approximant in Theoretical Physics*, edited by G. A. Baker, Jr. and J. L. Gammel (Academic, New York, 1970).
- ³⁶See, e.g., M. E. Fisher and H. Au-Yang, *J. Phys. A* **12**, 1677 (1979).
- ³⁷P. Seglar and M. E. Fisher, *J. Phys. C* **13**, 6613 (1980).
- ³⁸D. F. Styer and M. E. Fisher, in *Rational Approximation and Interpolation, Lecture Notes in Mathematics*, edited by P. R. Graves-Morris, E. B. Saff, and R. S. Varga (Springer, Heidelberg, 1984), Vol. 1105, pp. 313–330.
- ³⁹(a) M. E. Fisher and D. F. Styer, *Proc. R. Soc. London, Ser. A* **384**, 259 (1982); (b) D. F. Styer and M. E. Fisher, *ibid.* **388**, 75 (1983); (c) D. F. Styer, *ibid.* **390**, 321 (1983).
- ⁴⁰M. Randeria and M. E. Fisher (unpublished).
- ⁴¹J. Nuttall, *J. Approx. Theory* **42**, 299 (1984).
- ⁴²L. P. Kadanoff and H. Ceva, *Phys. Rev. B* **3**, 3918 (1971).
- ⁴³M. Barma and M. E. Fisher, unpublished PDA study of the Ising model for general spin S .
- ⁴⁴A. D. Bruce, *J. Phys. C* **14**, 3667 (1981).
- ⁴⁵M. E. Fisher and J.-H. Chen (unpublished).
- ⁴⁶(a) M. Blume, *Phys. Rev.* **141**, 517 (1966); (b) H. W. Capel, *Physica* **32**, 966 (1966).
- ⁴⁷In terms of the customary nearest-neighbor exchange coupling J and crystal-field term Δ , the parameters in (6.6) are given by $w = [1 + \frac{1}{2} \exp(\Delta/k_B T)]$ and $\hat{K}(0) = qJ/yk_B T$, where q is the coordination number of the lattice.
- ⁴⁸W. Selke, D. A. Huse, and D. M. Kroll, *J. Phys. A* **17**, 3019 (1984).
- ⁴⁹(a) M. P. M. den Nijs, *J. Phys. A* **12**, 1857 (1979); (b) R. B. Pearson, *Phys. Rev. B* **22**, 2579 (1980); (c) D. P. Landau and R. H. Swendsen, *Phys. Rev. Lett.* **46**, 1437 (1981).